May 1, 2008

Austin Folley, Emma Setterington, David You

University of Arizona

Dr. Jeong-Yeol Yoon
403 Shantz
University of Arizona
Tucson, AZ 85721

CC: Dr. Muluneh Yitayew
533 Shantz
University of Arizona
Tucson, AZ 85721

Dear Dr. Yoon,

We are pleased to submit to you this final report detailing the design of a portable biosensing device for the detection of *E. coli* in water. You commissioned us with this project in November 2007, and we have completed it prior to the deadline of May 1, 2008.

The system under design is intended to meet the following criteria:

- Device is fully portable
- Operation is simple and interface is user-friendly
- Results are accurate and performance is consistent
- Response time is short
- Cost is minimized

This report describes the public need for such a device, the objectives of our work, and the theory by which the system operates. It then discusses the alternative solutions considered and describes our design approach and the final prototype in detail. We also provide you with some preliminary experimental results, comments on ethical considerations, an economic analysis, and recommendations for continuation of the project. We hope that you will find our design to be innovative, useful, and well-presented. Thank you for allowing us to work with you, and please do not hesitate to contact us with any questions or concerns.

Sincerely,

Austin Folley Emma Setterington David You

A PORTABLE BIOSENSING DEVICE FOR THE DETECTION OF *ESCHERICHIA COLI* IN WATER

Project Team: Austin Folley
Emma Setterington
David You
Department of Agricultural & Biosystems Engineering
The University of Arizona

Project Advisor: Dr. Jeong-Yeol Yoon

Course Instructor: Dr. Muluneh Yitayew, ABE 498

May 1, 2008

A PORTABLE BIOSENSING DEVICE FOR THE DETECTION OF *ESCHERICHIA COLI* IN WATER

ABSTRACT

Escherichia coli O157:H7 is nationally one of the leading causes of foodborne disease, and is acquired primarily through consumption of undercooked beef or unwashed vegetables (CDC, 2006). Many biosensors have been designed which are capable of accurate *E. coli* detection and quantification, but a great need remains for a sensing device which can monitor food quality directly *at the point of contamination*, that is, on farms or in processing facilities. A fully portable, hand-operated biosensing instrument has been designed for this purpose. Its immunoaffinity sensing element utilizes antibody-coated microscale particles, which agglutinate in the presence of the target bacteria. Its optical transducing element uses a photodetector to measure light scattered by agglutinated particles. The instrument has a simple, user-friendly interface and can be easily operated by non-technical personnel. Quantitative results are quickly and clearly displayed on an LCD screen built into the device. Minor adaptations to this system can make it sensitive to target compounds other than *E. coli*, for a broader range of practical applications.

KEY WORDS

Portable, biosensor, *E. coli*, optical, light scattering, photodiode

ACKNOWLEDGEMENTS

Our project team would like to thank Dr. Jeong-Yeol Yoon for directing us toward our project goal and for his expertise in lab-on-a-chip and optical technology, his thorough and clear explanations of the scientific theory, and his insightful input into our design.

We would also like to thank Brian Heinze and Jin-Hee Han, graduate researchers in the University of Arizona Biosensors Laboratory, for demonstrating lab-on-a-chip experiments and teaching us the related laboratory procedures.

Finally, we thank Dr. Muluneh Yitayew for his instruction.

TABLE OF CONTENTS

List of Figures 1
List of Tables 3
Introduction 4
Objectives 8
Specifications 8
Background & Theory: Biological Sensing and Optical Detection 9
Alternative Design Solutions 11
  Light Source 11
  Positioning Mechanism 12
  Light Detector 14
  Signal Processor and Display 16
  Final Selection 18
Approach 19
  Circuit Design 19
  Structural Design & Prototype Development 31
  Experimentation & Results 37
Ethical Considerations 38
Economic Analysis 39
Conclusions & Recommendations 42
References 44
Appendix A: Design Criteria & Constraints 45
Appendix B: Materials List & Prototype Parts 47
Appendix C: Experimental Results 53
Appendix D: Economic Calculations 55

LIST OF FIGURES

Figure 1. The "Seven Sensor," part of a continuous blood glucose monitoring system (DexCom™, Inc 2007).

Figure 2. SPIRIT portable detection system (Seattle Sensor Systems, Inc. n.d.).

Figure 3. RAPTOR portable biosensor unit (Research International, Inc 2007).

Figure 4. Transmission Electron Micrograph photo of *E. coli* (source: New York State Department of Health).

Figure 5. The "PDS Solution" automated desktop testing unit for *E. coli* detection in water (Pathogen Detection Systems, Inc. 2004-2006).

Figure 6. Immunoagglutination of antibody-conjugated microparticles and target bacteria (Yoon, 2007).

Figure 7. Optical measurement of immunoagglutination: focused light is scattered when it strikes clumped particles in the sample solution.

Figure 8. Two-well glass slides (image source: Microscope-Depot.com).

Figure 9. Two-well slide platform in use for lab-on-a-chip assay. One well contains a blank solution; the other contains the liquid sample being tested (Lucas et al., 2007).

Figure 10. Laboratory light source module (Ocean Optics, 2007).

Figure 11. Circuit diagram notation for an LED.

Figure 12. Laser diodes (image source: edmundoptics.com).

Figure 13. Example of rack and pinion adjustment mechanism: when knob is turned, slide moves laterally.

Figure 14. Ocean Optics USB4000 spectrometer (Ocean Optics, 2007).

Figure 15. Top, avalanche photodiode (image source: edmundoptics.com); bottom, circuit diagram notation for photodiodes.

Figure 16. Operation of a PMT (image source: Florida State University).

Figure 17. A typical voltmeter module (Martel, 2007).

Figure 18. Microchip Technology PICkit™ (Microchip, 2007).

Figure 19. Diagram of photo-detecting circuit.

Figure 20. Stage 1 – APD light detection.

Figure 21. Stage 2 – Differential Op-amp.

Figure 22a. Example of a non-inverting circuit configuration for an op-amp.

Figure 22b. Example of an inverting circuit configuration for an op-amp.

Figure 23. Stage 3 – Zero Adjust.

Figure 24. Stage 4 – Gain Stage.

Figure 25. Stage 5 – PIC Microcontroller.

Figure 26. Stage 6 – LCD Display

Figure 27. Photograph of initial circuit, assembled on breadboard.

Figure 28. Second version of circuit, front (left) and back (right).

Figure 29. Third version of circuit, front (left) and back (right), shown without components.

Figure 30. Fourth version of circuit, front (left) and back (right).

Figure 31. Photoshop design for fifth version of circuit, front (left) and back (right).

Figure 32. Preliminary construction of fifth circuit on a breadboard.

Figure 33. Fifth and final version of circuit, front (left) and back (right).

Figure 34. Completed housing with components.

Figure 35. Open and closed positions of sliding tray mechanism.

Figure 36. Side view of housing, showing power supply access.

Figure 37. Top view of housing, with LCD interface.

Figure 38. Aluminum sheet attaching PIC microcontroller to inner lid of housing.

Figure 39. Support complex for the APDs and laser diodes; (a) disassembled and (b) assembled.

Figure 40. Assembled support complex, holding laser diodes and APDs, in place within the housing.

Figure 41. Completed housing, closed position.

Note: Any figures without a source provided were created by the authors of this report.

LIST OF TABLES

Table 1. Comparison of two alternative light sources.

Table 2. Comparison of alternative mechanisms for positioning the two-well slide.

Table 3. Comparison of alternative light detecting components.

Table 4. Comparison of alternative components for signal processing and display.

Table 5. Selected solution for each of the essential functions in our design, and justification for each selection. Table 6. Results of statistical t-tests.

Table 7. Itemized costs for materials and construction of prototype device.

Table 8. Costs associated with operation of device.

INTRODUCTION

In recent years, the rapidly expanding field of biosensor research and design has produced literally dozens of sensors utilizing novel, rapid detection methods. Biosensors can detect anything from microorganisms and cells to viruses, proteins, chemicals and toxins. Typically, the target compound is captured by antibody-antigen binding, enzyme-substrate binding, or nucleic acid base-pairing. Capture of the target initiates a response in the sensor that can be conventionally measured, such as a change in the electrical, chemical, structural, or optical properties of the substances involved.

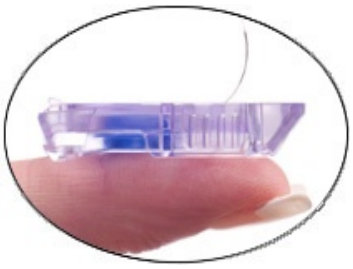

Figure 1. The "Seven Sensor," part of a continuous blood glucose monitoring system from DexCom™ (DexCom™, 2007).

Biosensor technologies have the potential to revolutionize medicine, homeland security, sanitation, food safety, and military operations. Diagnostics and substance identifications which formerly required extensive time and labor can now be carried out in a matter of minutes, with the right equipment. A few types of biosensors, such as those produced by DexCom™ (Figure 1; DexCom™, 2007) and Medtronic (Medtronic, 2007) for continuous monitoring of blood glucose, have reached the market and are widely used by both commercial and individual consumers. However, the vast majority of biosensors are still limited to laboratory use by select personnel. In order to take full advantage of these new, powerful sensing capabilities, focus must be directed toward making them portable, simple to use, and field-functional.

Figure 2. SPIRIT portable detection system (Seattle Sensor Systems, n.d.).

Although the vast majority of biosensor research is geared toward initial development of novel sensors, a number of portable biosensor systems do exist which are compact and intended for field detection. One of the commercially available portable sensing systems is the "SPIRIT," or Surface Plasmon Instrumentation for the Rapid Identification of Toxins, developed and sold by Seattle Sensor Systems (Seattle Sensor Systems, n.d.). Surface Plasmon Resonance (SPR) is a common biological detection technique. This unit can

screen for up to 24 different substances simultaneously. The entire experimental setup, including sensors, reagents, automated fluidics, optical equipment, a built-in touch-screen LCD with custom software, and power supply, is contained and functional within a single carrying case (Figure 2).

Figure 3. RAPTOR portable biosensor unit (Research International, 2007).

Research International, another company based in Seattle, has developed and produced a biosensor system called the RAPTOR (a Rapid, Automatic, and Portable Fluorometer Assay System). This unit can screen for four substances simultaneously, and it functions by measuring light emitted from fluorescently-labeled antibodies, in order to indicate presence of the target. Once again all of the sensing and processing equipment is combined into one compact case, shown in Figure 3 (Research International, 2007).

The majority of portable biosensor systems in existence have been created by researchers but never optimized and commercially produced. It is clear that out of the vast field of biosensors, few are equipped for real-world field applications.

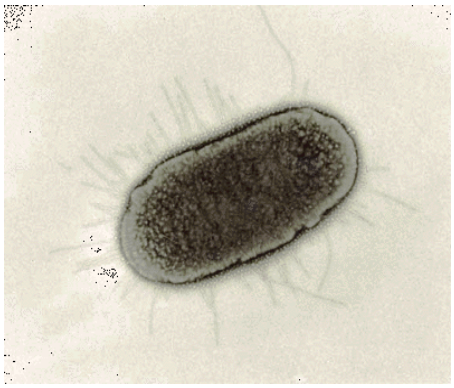

Figure 4. Transmission Electron Micrograph photo of *E. coli* (image source: New York State Department of Health).

In view of this need, we have undertaken to design a portable sensing system for detection of *Escherichia coli*, a common bacterium (Figure 4). *E. coli* naturally inhabits the intestines of both humans and animals, and plays an essential role in digestion. While most *E. coli* are harmless and even helpful, certain strains can be deadly. In particular, the *E. coli* strain O157:H7 is one of the largest causes of foodborne disease in humans. While less serious strains of *E. coli* can cause symptoms such as diarrhea, abdominal pain, fever, and vomiting when consumed in significant quantities, the most severe effect of the strain O157:H7 is Hemolytic Uremic Syndrome

(HUS). This often results in death due to kidney failure and the destruction of red blood cells and platelets (Marler-Clark, 2007; CDC, 2006).

E. coli is typically acquired through consumption of undercooked beef, unwashed vegetables, or contaminated water. Because large amounts of *E. coli* live in the intestines of animals, including strains such as O157:H7 which are pathogenic to humans, it is possible for meat to come in contact with these bacteria during the slaughtering process. Thorough cooking is necessary to kill the pathogens. Additionally, *E. coli* is found in large quantities in the fecal matter of animals and humans. Plant crops can be exposed to *E. coli* via manure fertilizers or contaminated irrigation water, and become a source of foodborne disease if the crops are consumed without proper cleaning. Bodies of water which are tainted with sewage will also contain high *E. coli* levels, and will spread disease if used for drinking or washing (Marler-Clark, 2007; CDC, 2006).

The Center for Disease Control and Prevention has estimated that 73,000 Americans are infected by *E. coli* annually, of which 2,100 are hospitalized. While measures have been taken to prevent the spread of *E. coli*, outbreaks still occur (CDC, 2006). In fact, the most recent *E. coli* outbreak was in October 2007, and was caused by contaminated ground beef.

Attempts to prevent the spread of foodborne disease include regularly testing water sources, produce, and meat for dangerously high *E. coli* levels. Typical tests require a laboratory facility and skilled personnel, and may take as long as forty-eight hours to obtain results. This waiting period is often too long for a test to be of use, because processing and sale of fresh foods is highly time-sensitive.

There is obviously great demand for the design and commercialization of a field-ready biosensor that can quickly measure of *E. coli* levels with the same sensitivity and accuracy as laboratory analysis. Pathogen Detection Systems Inc. is a company seeking to fulfill this demand, and is in the process of commercializing an automated *E. coli* water detection system. Their design, dubbed the "PDS Solution," consists of a desktop unit (Figure 5)

which connects to a computer for processing and display of results. The fluid sample is put into a disposable test cartridge containing reagents. Enzymes produced by *E. coli* or other coliform bacteria which are present in the sample react with these reagents to form a fluorescent product. The product accumulates in a film on one end of the cartridge, where it is excited by a light source and the subsequent fluorescence is detected by a spectrometer. Because of the required incubation time, a single test using this device may take 6-16 hours to complete (Pathogen Detection Systems, 2004-2006).

Figure 5. The "PDS Solution" automated desktop testing unit for *E. coli* detection in water (Pathogen Detection Systems, 2004-2006).

While the "PDS Solution" provides results more quickly than traditional laboratory tests and is somewhat portable, it leaves several things to be desired. For a system to be truly suited for use in the field, it must be totally self-powered, easy to transport, and able to produce results in a matter of minutes rather than hours.

In order to meet the demand for a completely field-functional system for *E. coli* testing, we will design a biosensing device based on microscale methods of biological detection and signal transduction. We will utilize immunoaffinity sensing and optical transduction techniques which have been developed in part by our client, Dr. Jeong-Yeol Yoon, in the biosensors laboratory at the University of Arizona. Because the detection process is carried out on such a small scale, our system will be contained in a single unit which can be easily carried and operated by one person. We will also design our sensing device to have a quick response time, a simple user interface, and a reasonable production cost, so that our final product will be truly marketable and beneficial to the field of food safety, and beyond.

OBJECTIVES

In order to develop a new, fully-portable biosensing device for the detection of waterborne *E. coli*, based on immunoaffinity sensing and optical transduction, the following objectives must be completed:

- Selection of components to function as light source, light detector, internal processing unit, and power supply;
- Design of electrical circuit to connect and support these components;
- Structural design of housing and mechanical positioning elements;
- Construction of fully functional prototype device;
- Experimental data collection and appropriate programming of internal processor.

SPECIFICATIONS

Our client, Dr. Jeong-Yeol Yoon, has requested the design of a biosensing device based on antibody-antigen affinity and optical detection of scattered light. The intended purpose of this device will be to monitor *E. coli* levels in public water sources, natural bodies of water, and commercial or agricultural water supplies. The design specifications outlined by our client are as follows:

- System is fully portable
- Operation is simple and interface is user-friendly
- Results are accurate and performance is consistent
- Response time is short
- Cost is minimized

For a more detailed explanation of the criteria and constraints adhered to by the designers, please see Appendix A.

BACKGROUND & THEORY - *Biological Sensing and Optical Detection*

Our design will utilize the sensing and transduction techniques which have been developed by our client's research group for use in lab-on-a-chip biosensors. The immunoaffinity sensing element functions as follows: Tiny latex microparticles, only 0.92 microns in diameter, are coated with antibodies specific to the target bacterium. This microsphere conjugate is combined with the sample fluid being tested. When the target bacterial species is present in the sample, its attraction to the antibodies will cause the microparticles to adhere to one another, forming doublets or larger clumps. This phenomenon is called immunoagglutination (Figure 6).

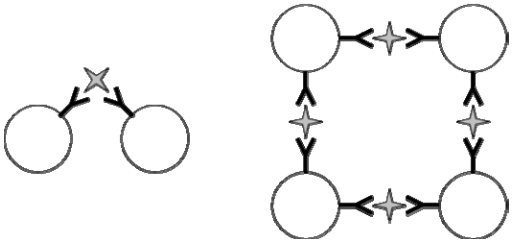

Figure 6. Immunoagglutination of antibody-conjugated microparticles and target bacteria (Yoon, 2007).

Immunoagglutination greatly increases the average particle size in the sample solution. The extent of agglutination is determined optically, by directing a light beam through a small volume of the solution and measuring the intensity of scattered light. This optical measurement is conceptually depicted in Figure 7. The extent of light scattering is directly correlated to particle size, which is dependent on the quantity of target bacteria present in the sample. Our client's research group has demonstrated successful use of this technology in the laboratory with the lab-on-a-chip microfluidic device, achieving detection of *E. coli* at levels as low as 40 colony forming units (CFU) per ml. The majority of contemporary biosensors for *E. coli* have detection limits greater than 100 CFU/ml, showing the lab-on-chip methodology to be a truly superior sensing technique (Han et al., 2008).

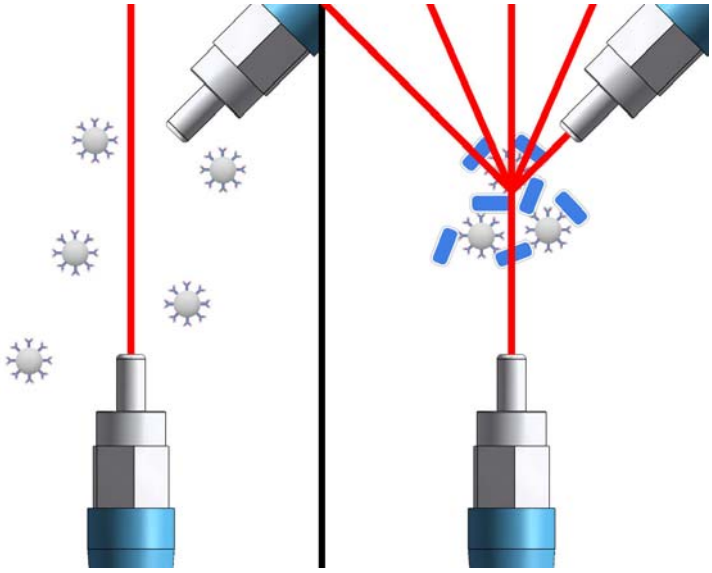

Figure 7. Optical measurement of immunoagglutination: focused light is scattered when it strikes clumped particles in the sample solution.

The immunoagglutination and optical detection assay can be carried out on various platforms. Although the lowest detection limit was achieved using a microfluidic platform with pressure-driven flow through enclosed channels, we have opted to use a simple glass slide with two indented wells (Figures 8 and 9) as the assay platform in our portable device. The two-well slide platform greatly reduces the complexity of the system, while preserving functionality and accuracy.

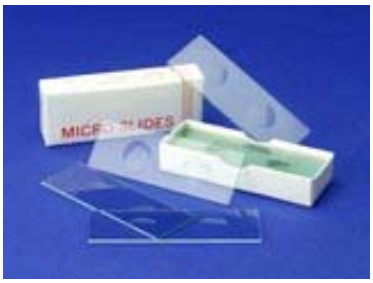

Figure 8. Two-well glass slides (image source: Microscope-Depot.com).

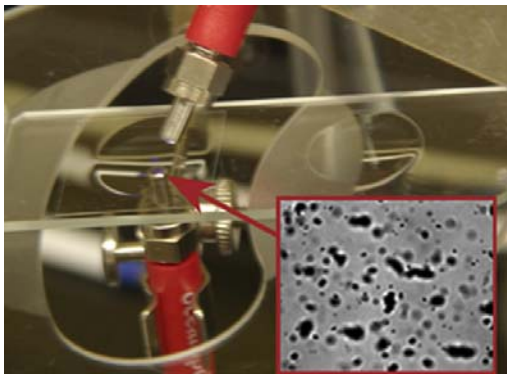

Figure 9. Two-well slide platform in use for lab-on-a-chip assay. One well contains a blank solution; the other contains the liquid sample being tested (Lucas et al., 2007).

Before an unknown sample is tested using this technique, a measurement must first be taken of a blank sample, that is, a buffer solution containing antibody-coated particles but none of the target bacteria. The intensity of scattered light for the blank is compared with that of the real sample (which may contain the target bacteria), and the difference between the two values indicates the quantity of target bacteria present in the sample.

ALTERNATIVE DESIGN SOLUTIONS

Our portable device for *E. coli* detection will utilize antibodies to trap bacterial cells from a liquid sample and form clumps of particles (immunoagglutination). The extent of immuno-agglutination will be detected by emitting a light beam through the solution and measuring the resultant scattering of light, due to photons striking the particles and being deflected.

In the interest of making our device as compact, simple to use, and economical as possible, we intend to eliminate the bulky and expensive equipment which is utilized for optical detection in the laboratory. The current laboratory setup includes a light source module, fiber optic cables, a finely adjustable x-y-z positioning stage, a small spectrometer, and a desktop computer equipped with custom software for display of results. Most of these instruments must be plugged into a wall outlet for power. The entire arrangement requires as large, flat working area and takes up a great deal of space. The detection platform and adjacent fiber optic cables must be precisely positioned and not physically disturbed at all during experimentation.

We have evaluated a number of alternative components and mechanisms which could be employed to function as the light source, positioning mechanism, light detector, signal processor and display. Below we discuss these options and the benefits or drawbacks to each.

- **LIGHT SOURCE**

The light source module used in the laboratory is the Ocean Optics LS-450 Blue Pulsed Light Source (Figure 10), costing $524 (Ocean Optics, 2007). One alternative light source that we have considered to replace this component is a light emitting diode (LED). LEDs are the familiar little lights often found in remote controls, stereos, and other electrical devices, and they are simply diodes which emit a spectrum of light when exposed to an electrical current.

Figure 10. Laboratory light source module (Ocean Optics, 2007).

Diodes are generally thought of as a "check valve" allowing current to flow in one direction (forward bias) but not in the opposite direction (reverse bias), and the most common diodes are made from a semiconductor material such as silicon. The LED works in the same manner as the diode; however, when current flows in the forward bias direction of the LED, light is emitted. In standard circuit diagrams, the LED is depicted as shown in Figure 11.

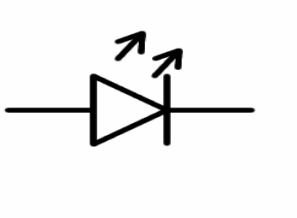

Figure 11. Circuit diagram notation for an LED.

Figure 12. Laser diodes (image source: edmundoptics.com).

A second component which could replace the laboratory light source module is a laser diode (Figure 12). It is composed of a semiconductor material like an LED, yet functions in a slightly different way. When current runs through an LED, lattice vibrations cause energy to be released in the form of phonons. When passing current through a laser diode, photons are released via spontaneous emission, creating a much stronger, more intense signal than the LED. Table 1 compares the pros and cons of the LED versus the laser diode.

Table 1. Comparison of two alternative light sources.

Alternatives for Light Source	Benefits	Drawbacks
Light Emitting Diode (LED)	Very small, cheap, long lasting, variety of sizes & wavelengths	Unfocused light, low intensity
Laser Diode	Focused beam, high intensity	Larger and much more costly

- **POSITIONING MECHANISM**

When laboratory tests are carried out on a two-well slide, the blank solution is put into one well and the sample is put into the other. The slide is placed between the light source and the light detector, and adjusted to ensure that the beam of light strikes the center of the well. After measuring the blank, the slide must be repositioned laterally so that the other well is in place for measurement. This requires either a large range of motion on the positioning stage, or human contact to manually move the slide.

For our portable system, we want to decrease the risk of system damage and error in results by minimizing user contact with the components. The entire system will be enclosed and measurements will be taken inside the housing, protected from ambient light and from inadvertent disturbances. The slide will rest on a tray that slides in and out of the housing like a drawer, and in when the drawer is the "closed" the slide will be positioned directly above the light source and directly beneath the light detector. However, we must still provide a means for measurements to be taken of both wells in the slide, and for the well to be centered precisely over the light beam. We considered two primary ways to achieve this.

Our first option is to have the slide secured into a rack and pinion system on the tray, so that the user can control the lateral motion of the slide inside the housing, simply by turning an external knob (Figure 13). A rack and pinion mechanism could feasibly be used for both fine position adjustment, and for switching between one well and the other. The major downside to this option, however, is that measurements of the blank and the sample would be taken one after another. This would require a processor advanced enough to store one value while measuring the next, and then subtract the first (blank) from the second (sample) and output this difference. The computer and software utilized in the laboratory can do this easily, but we intend to use a small, inexpensive, and self-programmed processor which will most likely not possess internal memory. So this option would add much complexity to the processing element of our design.

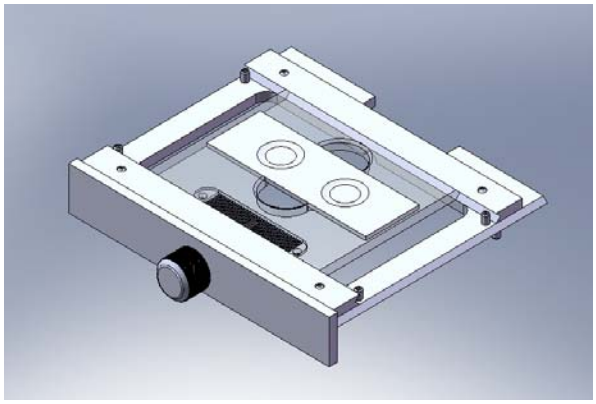

Figure 13. Example of rack and pinion adjustment mechanism: when knob is turned, slide moves laterally.

Secondly, we considered employing two light sources and two light detectors in our device, one set for each well of the slide. This way the measurements of the blank and the sample can be taken simultaneously so that the slide does not need to be move from one side to the other, and also the need for an advanced processor is eliminated. In order to ensure that the wells are placed precisely, we propose making the light sources and detectors position-adjustable rather than the slide. The slide can be held stationary in a fixed indentation on the

tray so that no "accidental" position adjustments can be made. Before the initial use of the device, and for periodic calibration, however, the housing must be opened to allow correct positioning of the light sources and detectors relative to the internal position of the slide. Then these components will be anchored into place and are not likely to be disturbed again within the closed housing. The only downside we see to this arrangement is that the duplicate components would add to the cost of the device. A summary of alternative positioning mechanisms is shown in Table 2.

Table 2. Comparison of alternative mechanisms for positioning the two-well slide.

Alternatives for Positioning	Benefits	Drawbacks
Rack & Pinion Lateral Slide Adjustment Mechanism	Allows slide to move laterally so that either well can be positioned between the light source and detector; only one set of components required	Measurements taken one at a time, requiring advanced processing (blank value must be stored during second test, then subtracted from sample value)
Dual Light Sources and Detectors	Both wells of the slide have own light source and detector, for simultaneous measurements of blank and sample	Dual components add to expense

- **LIGHT DETECTOR**

The light detecting component used in the laboratory is the Ocean Optics USB4000 miniature spectrometer (Figure 14), costing $2309 (Ocean Optics, 2007). The simplest alternative light detector that we have considered is a photodiode, which is an electrical component that generates current when excited by incoming light. A traditional photodiode has two polarized legs, an anode and a cathode, and when these are wired into a circuit and the photodiode is illuminated by a light source, current will flow. Normally the intensity of incoming light and the corresponding outgoing current are linearly related.

Figure 14. Ocean Optics USB4000 spectrometer (Ocean Optics, 2007).

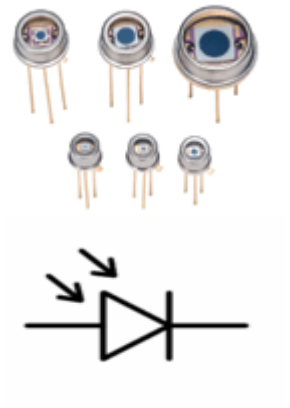

Figure 15. Top, avalanche photodiode (image source: edmundoptics.com); bottom, circuit diagram notation for photodiodes.

An avalanche photodiode or APD (Figure 15) has the ability to amplify or "avalanche" the generated current up to 100 times, using complex impact ionization effects. Just a few photons striking the APD can generate a substantial current. For example, if a regular photodiode produces a current of 0.01 mA when illuminated at a certain intensity, then an APD with a gain of 100 will produce a current of 1 mA under the same conditions, which is a much more readable signal. The standard notation for photodiodes in circuit diagrams is shown in Figure 15.

A second alternative light detector is the photomultiplier tube (PMT). Like an APD, a photomultiplier tube can amplify a weak incoming light signal to generate a strong current. While most APDs only produce a gain of around 100, high end PMTs are capable of multiplying the production signal by as much as 10^8 (Marmonier, 2002).

The principle and circuitry associated with the PMT is fairly complex, but underlying its operation are four main components: 1) a photocathode which converts light flux into electron flux; 2) an electron optical input system which focuses and accelerates the electron flux; 3) an electron multiplier consisting of a series of secondary emission electrodes (dynodes); and 4) an anode which collects the electron flux from the multiplier and provides the output signal (Marmonier, 2002). The amplification of a photon within a PMT is shown in Figure 16.

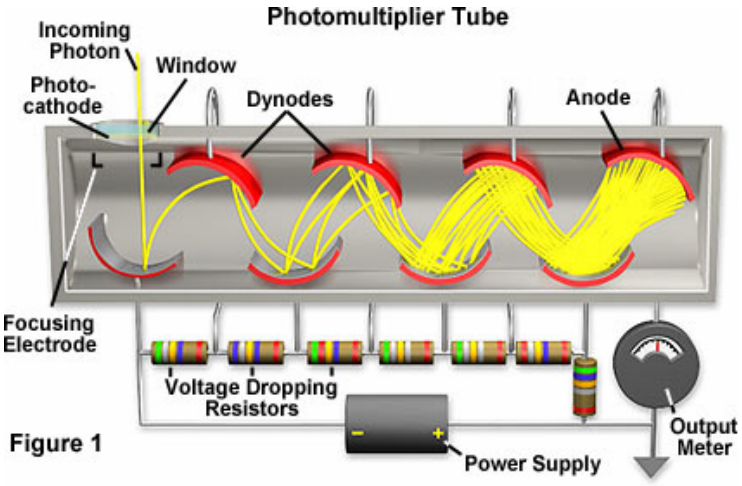

Figure 16. Operation of a PMT (image source: Florida State University).

Although PMTs offer extraordinary amplification and sensitivity compared to a photodiode or even an APD, they tend to be larger and more expensive, with prices ranging anywhere from hundreds to thousands of dollars. Table 2 compares the pros and cons of the alternative light detectors considered.

Table 3. Comparison of alternative light detecting components.

Alternatives for Light Detector	Benefits	Drawbacks
Photodiode	Small size, inexpensive (~$20), simple	Low sensitivity because no signal amplification ability
Avalanche Photodiode (APD)	Small size , has amplification ability (gain ~100)	Cost ~$100
Photomultiplier Tube (PMT)	Excellent amplification ability (gain ~10^8)	Larger, cost $500-$1000, consumes more power, requires more complex circuit

- **PROCESSOR & DISPLAY**

As mentioned previously, the laboratory setup depends on a computer and an expensive software package (SpectraSuite Spectroscopy Platform software from Ocean Optics) to perform the signal processing and display of results. The essential functions of the processor are to receive the incoming signals (current generated by the photo detectors due to scattered light), compute the difference (between blank and sample), and output this value on some sort of display. If the output were a raw voltage value, the user would need a table or equation by which to convert this value to the corresponding *E. coli* concentration. However, if the processor was programmable, it could be initially equipped with a program for this value conversion, and the display would show the value of the *E. coli* concentration rather than a voltage value. We have considered three options for processing and display of results.

Figure 17. A typical voltmeter module (Martel, 2007).

The first is a voltmeter module, a self-contained unit which includes an analog/digital converter, an LCD display, and all the necessary features for integration into an existing electrical system. A prime example is the Martel Meters SP400 Blue 3.5-

digit backlit LCD voltmeter module, shown in Figure 17 (Martel, 2007). The cost is approximately $50. A drawback to this option is that it can only display a limited range of voltage values, and cannot be programmed, so this would require the user to interpret the values on the display in order to obtain the actual cell concentration.

The next option considered is an analog/digital converter chip (ADC), which allows the analog input (voltage) to be converted to a binary output, which is then displayed on an LCD screen. The screen would be purchased separately and wired to the ADC. This chip is also not programmable, but unlike the voltmeter module, its display is not limited to a voltage reading. Instead, its range depends on the properties of the gain circuit and LCD display. Therefore, with an ADC, the circuit could be designed to do *some* manipulation of values prior to display, but nothing involving complex math. This would only be sufficient if the relationship between voltage signal and *E. coli* concentration is linear. The cost of an ADC plus an LCD screen is comparable to the cost of a voltmeter module.

Our third alternative for processing and display is a PIC, or "Programmable Intelligent Computer." This refers to a family of microcontrollers introduced by Microchip Technology, Inc. With an integrated 8-bit CPU (central processing unit), and data space in the form of RAM, PICs can be programmed to perform a wide variety of operations. Depending on the PIC, programming can vary from 35 instructions for low-end PICs, to 70 instructions for high-end PICs. Microchip Technology Inc. offers a PIC kit (Figure 18) providing a microcontroller and everything else needed for interfacing and programming it, for approximately $200 (Microchip, 2007).

Figure 18. Microchip Technology PICkit™ (Microchip, 2007).

A PIC microcontroller is the most powerful solution. It can read signal inputs, process them, and output the signal to an LCD. The major benefit of a microcontroller is that it can be programmed to carry out complex mathematical operations. However, the microcontroller

does require additional effort in programming and assembly. Table 3 compares the pros and cons of the alternative processors considered.

Table 4. Comparison of alternative components for signal processing and display.

Alternatives for Processing and Display	Benefits	Drawbacks
Voltmeter Module	Low cost (~$50), simple to implement	Display is limited to voltage; user must convert to cell concentration
Analog/Digital Converter plus LCD	Low cost (~$50), simple to implement	Could only display cell concentration IF relationship is linear, and would require more complex circuit
PIC Microcontroller	Can internally convert voltage value to display cell concentration	Most expensive ($200), requires assembly and programming

- **FINAL SELECTION**

After researching a great deal of alternative solutions for a light source, positioning mechanism, light detector, and signal processor, we narrowed down the list to only those few options described above. Weighing the positive and negative aspects of each, and taking into consideration their compatibility with the other selected components, we selected what we felt was the best solution for each necessary function. The chosen solutions, along with a brief justification for the selection of each one, are displayed in Table 5.

Table 5. Selected solution for each of the essential functions in our design, and justification for each selection.

FUNCTION	ALTERNATIVES	SELECTION	JUSTIFICATION
Light Source	• Light Emitting Diode (LED) • Laser Diode	**Laser Diode**	Since a highly focused light beam is required, a laser is the only feasible option.
Positioning Mechanism	• Rack & pinion lateral slide adjustment • Dual light sources and detectors	**Dual light sources and detectors**	This solution requires the least amount of user contact and eliminates the need for processor to have memory.

Light Detector	• Photodiode • Avalanche Photodiode (APD) • Photomultiplier Tube (PMT)	**Avalanche Photodiode**	The APD can significantly amplify a signal, making it much more sensitive than a photodiode, but still more affordable than a PMT.
Processor & Display	• Voltmeter Module • Analog/Digital Converter plus LCD • PIC Microcontroller	**PIC Microcontroller**	The PIC can be programmed to output the *E. coli* concentration value, regardless of relationship between voltage signal and concentration.

APPROACH

Our project was completed in five major phases, which were outlined in the *Objectives* section. After selecting the components and mechanisms by which the device will operate, the four remaining tasks were:

1) Design electrical circuit to support the components,
2) Design housing and mechanical positioning elements,
3) Construct prototype device,
4) Collect data and program the processor.

The following sections describe the approach taken to complete each of these tasks, the related theory, and the results.

- **CIRCUIT DESIGN**

The circuit we have designed to support photodetection for our experiments is shown in Figure 19. It consists of six different stages which act together to manipulate the incoming light signal. The circuit's final output is an expression of the concentration of *E. coli* in the water sample being tested in CFU/ml (colony-forming units per milliliter).

To better understand the circuit these six stages will be analyzed and discussed: 1) APD signal detection 2) Differential op-amp 3) Zero-adjust 4) Gain 5) PIC microcontroller 6) LCD display.

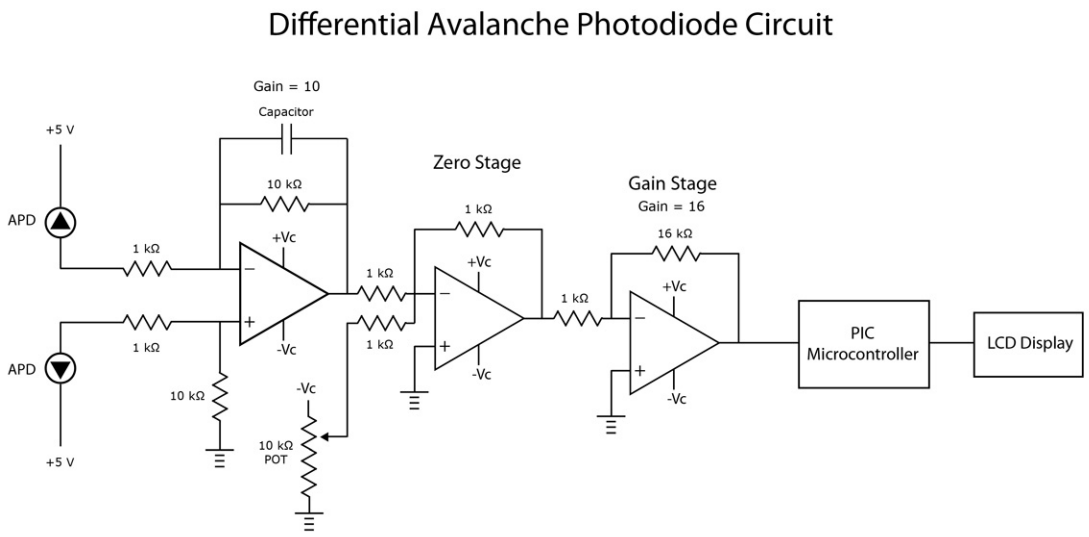

Figure 19. Diagram of photo-detecting circuit.

The first part of the circuit may be thought of as the sensor or the APD signal detection stage (Figure 20). This part of the circuit is responsible for detecting the light which is scattered by clumped particles in the water sample (after being emitted from the laser diodes beneath the samples). Specifically, the light signal enters through a small aperture on the face of the APDs, generating a current proportional to the light intensity throughout the circuit, which in turn produces a readable voltage. It is important to note that a voltage source of 5 V must be applied to each of the APDs in order to produce a measurable current. Without this voltage source, the amount of light entering the APDs would not produce a current large enough to be measured; however, with this voltage, the detected light acts similarly to a switch, "turning on" the circuit and "flooding" it with current.

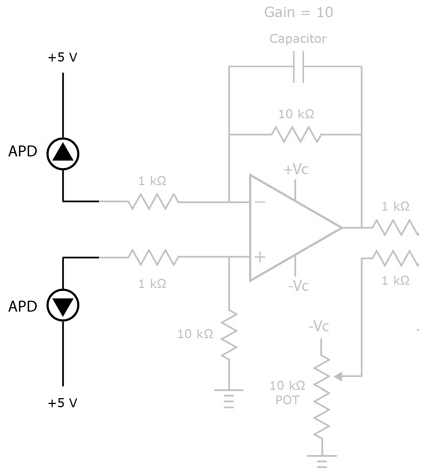

Figure 20. Stage 1 – APD light detection.

The second aspect of the circuit is the differential op-amp stage (Figure 21). While this stage may look complex, it is only performing simple subtraction. It is called *differential* because it is taking the difference of the two voltage signals coming from each of the photodiodes. *Op-amp* refers to the triangle shaped operational amplifier that subtracts the two signals.

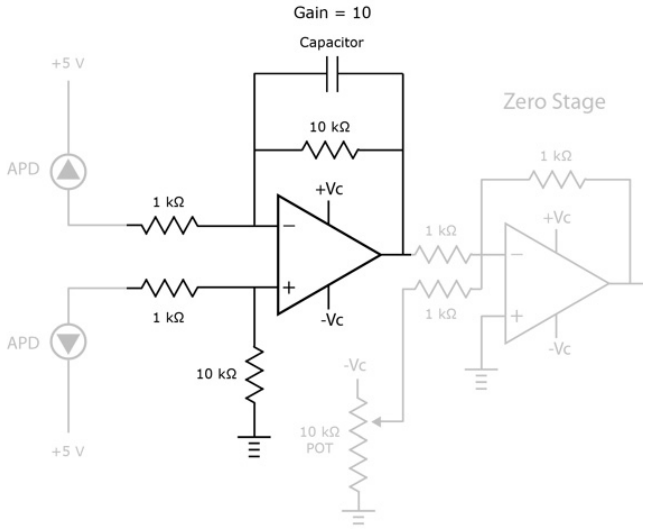

Figure 21. Stage 2 – Differential Op-amp.

An operational amplifier is best described as a solid-state integrated circuit which uses external feedback to control its functions. As evident by its name, the op-amp is capable of amplifying an input voltage signal, and the degree of amplification is dependent on the values of the resistors used in conjunction with the op-amp. A major benefit of using an op-

amp in a circuit is that it produces these voltage gains while drawing little or no current, and is therefore useful for protecting circuit components such as an APD.

There are two basic circuit configurations for op-amps. The first, a non-inverting configuration, is connected to the positive input terminal and does not change the sign of the signal (i.e., a positive input signal will produce a positive output signal). The second configuration, which is inverting, is connected to the negative input terminal and produces an inversion or a change in the sign of the output voltage (i.e., a positive input signal will result in a negative output signal). An example of circuits configured with inverting and non-inverting inputs are shown below (Figure 22a & 22b).

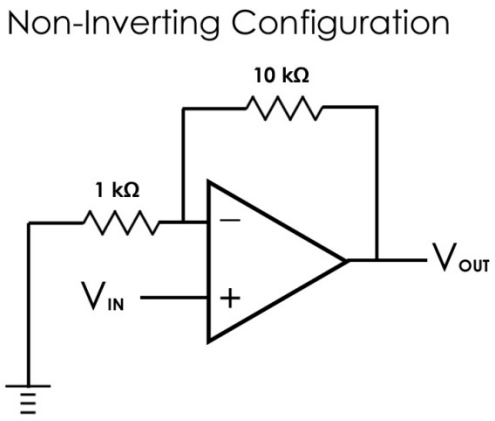

Figure 22a. Example of a non-inverting circuit configuration for an op-amp.

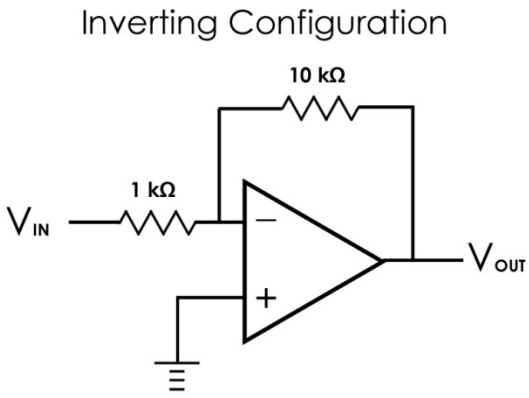

Figure 22b. Example of an inverting circuit configuration for an op-amp.

To understand the function of an op-amp, consider the non-inverting op-amp configuration from Figure 20a, for example. In this particular configuration, there are two resistors with values of 1 kΩ and 10kΩ. For an op-amp with a non-inverting configuration, the basic formula for determining the gain is:

$$gain = \frac{R_f}{R_i} + 1$$

Therefore in this example, the gain for the above circuit would be:

$$gain = \frac{R_f}{R_i} + 1 = \frac{10k\Omega}{1k\Omega} + 1 = 11$$

For an op-amp, the voltage output is related directly to the voltage input times the gain (V_{out} = *gain**V_{in}), and considering a theoretical voltage input of +0.5 volts for this example, the voltage output would be:

$$V_{out} = V_{in} \cdot gain = 0.5 \cdot 11 = +5.5V$$

The gain for an inverting op-amp circuit is derived in a similar manner for the non-inverting setup, but the two formulas are not exactly the same. For an inverting circuit setup, the equation for gain is:

$$gain = \frac{R_f}{R_i}$$

As an example, considering the inverting circuit provided in Figure 20b. R_f is equal to 10 kΩ and R_i is equal to 1 kΩ. Therefore, the gain for this circuit would be:

$$gain = \frac{R_f}{R_i} = \frac{10k\Omega}{1k\Omega} = 10$$

The output voltage (V_{out}) for the inverting configuration is found in the exact same way as the output voltage for the non-inverting circuit, except that there will be an inversion (change) in sign of the voltage. For example, a positive voltage will become negative and vice versa. Therefore, if a theoretical input voltage of +0.5 V is applied to the inverting circuit, the output voltage will be:

$$V_{out} = -V_{in} \cdot gain = 0.5V \cdot 10 = -5V$$

To understand how the differential op-amp setup in our circuit is working, consider one more example. If the APD connected to the positive terminal (+) of the op-amp produces a voltage of 50 mV while the APD connected to the negative terminal (-) of the op-amp produces a voltage of 30 mV, then a net voltage of 200 mV (that is, *gain*[50 – 30]*) will be output from the op-amp. The 10 kΩ and 1 kΩ resistors act as a positive gain (*gain = 10*) for the signal produced from the APDs and help to enhance the circuit's signal.

Following the differential op-amp setup is the zero-adjust stage (Figure 23) which is used to ensure a zero voltage output from the op-amp (the second op-amp in the circuit) if two *blank* samples are being tested.

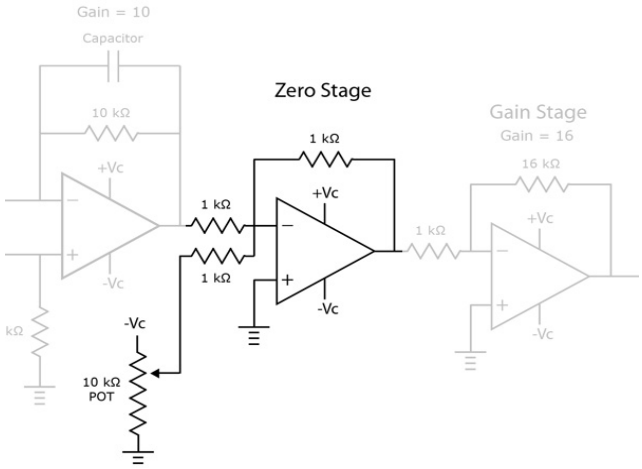

Figure 23. Stage 3 – Zero Adjust.

Recall that the *E. coli* detection tests involve a two-well slide with each well capable of holding approximately 80 µl of fluid. In order to properly run the tests and obtain a signal, one well must contain the water sample to be tested while the other well contains a buffer solution, or blank. (Remember that the signal obtained from the blank is subtracted from the signal of the water sample during the differential op-amp stage). Because the APDs being used are not absolutely identical and therefore may produce slightly different voltages given the same light input, this stage works to counter that problem and will therefore output 0 V any time a slide is tested containing two blank solutions. Unfortunately, the adjustments must be done manually, and they are made significantly easier with the help of the 10 kΩ potentiometer, seen in the figure. A potentiometer or "pot" is best thought of as an adjustable resistor, capable of creating a resistance up to 10kΩ. It is important to note that a negative voltage ($-V_c$) must be applied to the potentiometer in order to zero the signal. An example may best illustrate how this works.

Consider a two-well slide with each well filled with our standard buffer solution. Upon light scattering detection in stage 1, one APD produces a 30 mV signal while the other produces a 25 mV signal. After passing through the differential op-amp in stage 2, a signal voltage of 5 mV (30 – 25) will be output. Now, as the signal approaches stage 3, the potentiometer may

be used to create a -5 mV signal, and therefore generating an output of 0 V before passing onto the next stage. This stage is absolutely critical because the zero-volt signal will not allow the LCD in stage 6 to display an *E. coli* concentration when in fact there is no *E. coli* present in either well.

After the zero-adjust stage is the gain stage (Figure 24), which is used to amplify the voltage signal produced by the APDs. While the APDs do produce a stronger signal than a typical photodiode, they are still only producing voltages on the millivolt scale. The gain stage significantly amplifies the final output voltage by multiplying the signal received from the zero-adjust stage by a large constant.

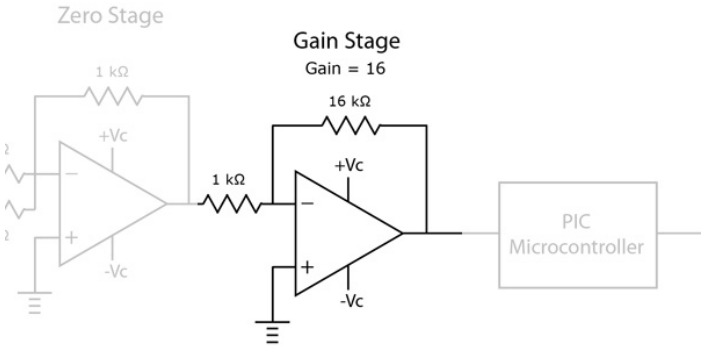

Figure 24. Stage 4 – Gain Stage.

As seen in Figure 24, the gain for the circuit is 16. The gain is determined by dividing the resistor value from the feedback loop (16 kΩ) by the resistor value from the branch leading into the negative input terminal (1 kΩ). Therefore, if a 0.2 V signal is output from the zero-adjust stage, a 3.2 V signal will be output at the end of the gain stage. A reading of 3.2 V is much easier to read and work with than a reading of 0.2 V, which is why this stage is so critical.

Stage 5 (Figure 25) involves the PIC microcontroller, which consists of a small circuit board with a programmable chip capable of taking an analog signal and converting it into a digital signal. Specifically, the microcontroller will take the final output voltage and, using the

analog to digital (A/D) converter, plug that value in to an equation that describes *E. coli* concentration as a function of the voltage signal. The equation is determined experimentally and programmed into the chip. Therefore the value output by the microcontroller is the actual concentration value of *E. coli* in the water sample.

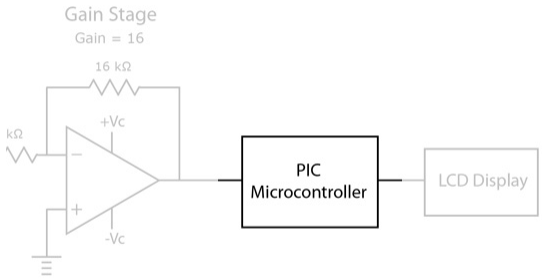

Figure 25. Stage 5 – PIC Microcontroller.

Finally, the PIC microcontroller also contains a built in LCD screen (Figure 26) for clear display of the final value.

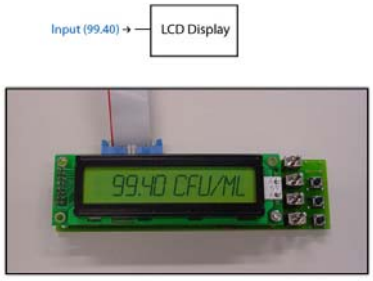

Figure 26. Stage 6 – LCD Display.

After the initial, theoretical design of the circuit on paper, our first physical version of it was created by assembling all the required components on a breadboard, which was connected to a power supply and ground (Figure 27).

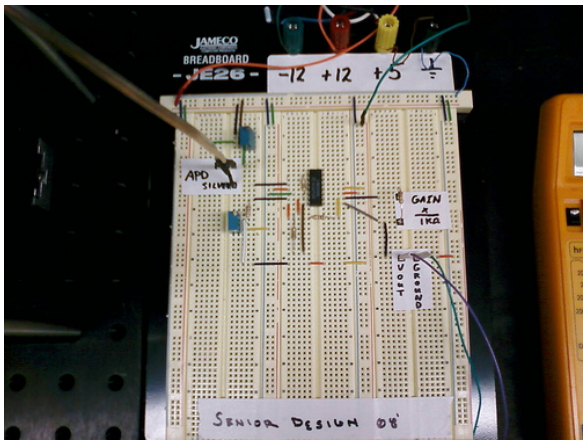

Figure 27. Photograph of initial circuit, assembled on breadboard.

After testing it out in the laboratory to ensure that our design was correct and everything was working properly, we constructed a second circuit that was identical but more compact (Figure 28). This version was built on a pre-drilled printed circuit board, so components were inserted on the front and had to be wired together on the back. Electrical "banana clips" were used for connections to the power source, ground, and APD. Although smaller than the breadboard, this circuit was still messy and prone to malfunction.

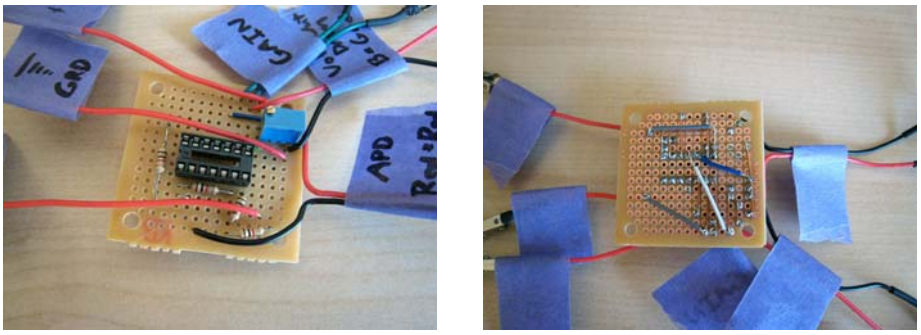

Figure 28. Second version of circuit, front (left) and back (right).

The third version of our circuit was significantly upgraded to a printed circuit board (Figure 29). The layout of this circuit was designed in Photoshop, printed, and ironed onto a copper-coated board to transfer the pattern. The board was then etched in ferric chloride solution to remove the copper from all areas except where it was protected by the transferred ink. A major downside to this design, however, is that vast areas of copper are etched away using a large amount of expensive ferric chloride solution.

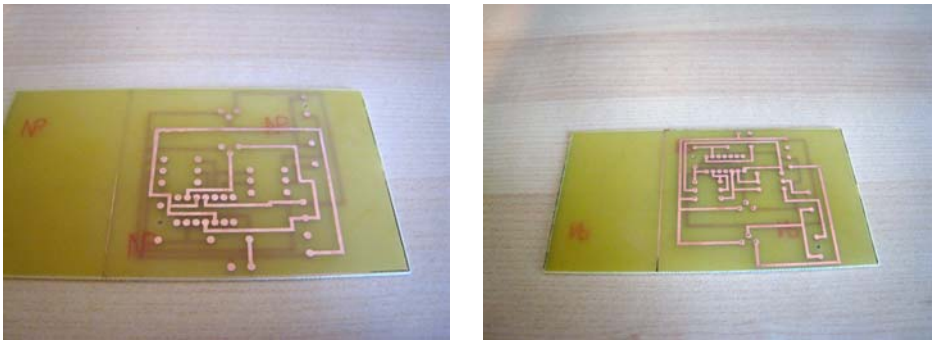

Figure 29. Third version of circuit, front (left) and back (right), shown without components.

The fourth version of our circuit was also on a printed circuit board (Figure 30), but was designed in such a way that much less etching solution was used, because copper was not removed from the entire board but only from those areas immediately surrounding the connections. This version also included some additional components between the power supply and the rest of the circuit: a 555 timer, diodes, and capacitors to output [(Vin-1)*-1)]. This way, if the power supply is providing +12 V, the circuit is receiving -11V, which is the correct power requirement for the op-amps and zero adjust potentiometer.

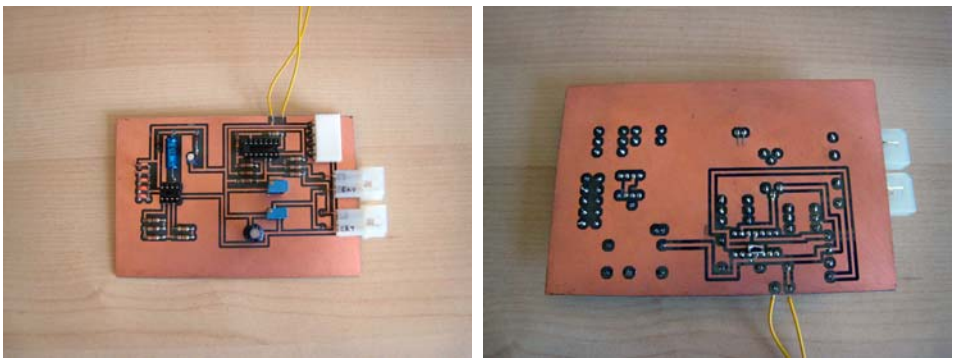

Figure 30. Fourth version of circuit, front (left) and back (right).

The Photoshop design of our fifth and final printed circuit is shown in Figure 31. The condensed grid at the bottom of the board can function as a sort of mini "breadboard," to allow components to be added without remaking the whole board.

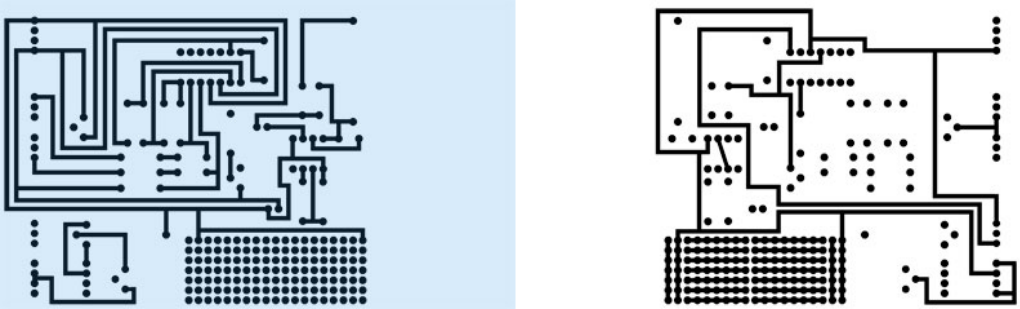

Figure 31. Photoshop design for fifth version of circuit, front (left) and back (right).

In addition to all the features of version four, this version also contains a relay switching and voltage regulation portion which will allow the laser diodes (used as the light source in our device) also to draw power from the circuit board. This circuit design was optimized to reduce overall size, achieving an approximate size reduction of 25% in compared to the previous version, even though the total number of components on the board was increased. We were able to conserve space by consolidating components; we replaced sets of resistors in series with single resistors of equivalent value, and we replaced multiple capacitors in parallel with a single equivalent capacitor.

Also in this final version, important resistors were added to the APDs and the grounds from the op-amp. The initial gain is 50 in the differential op-amp stage, and the final gain is 100 before the signal is sent to the microcontroller. Another key change to the circuit is that diodes were added in series with the output of the APDs running to the op-amp. This was done to counteract the op-amp's function of equalizing the inputs of the APDs at the positive and negative terminals before outputting the difference to the zero-adjust stage. The op-amp's attempts to equalize the APD inputs caused serious problems because when the output of one APD increased, the other increased as well, leading to errors in the voltage measurements and causing the circuit to behave unpredictably. By adding 1N4148 high-response, fast-switching diodes to our circuit, we were able to negate the undesired effect that the op-amp was causing on the APDs, and ensure that our circuit functioned properly and predictably. Figure 32 shows the construction and testing of this circuit on a breadboard, before it was etched and created on a circuit board. In this figure the laser diodes (green tape) are shown shining a light beam into the two APDs (purple tape), which are connected to the differential op-amp.

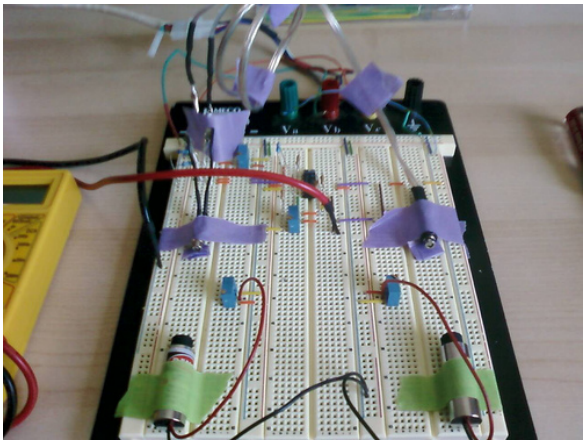

Figure 32. Preliminary construction of fifth circuit on a breadboard.

The circuit board construction of our final circuit is shown in Figure 33. The portion in the top left of the front view controls the laser diodes. The potentiometer regulates the voltage to the diodes and also allows for manipulation of the output intensity. There is a relay in the circuit that is connected to our PIC microcontroller. The relay turns on the circuit with the laser diodes whenever a voltage greater than 3.8 V is applied. We can connect this relay to an output on the PIC microcontroller so that the laser diodes can be turned on only when testing, thereby reducing power consumption and heat degradation to our samples.

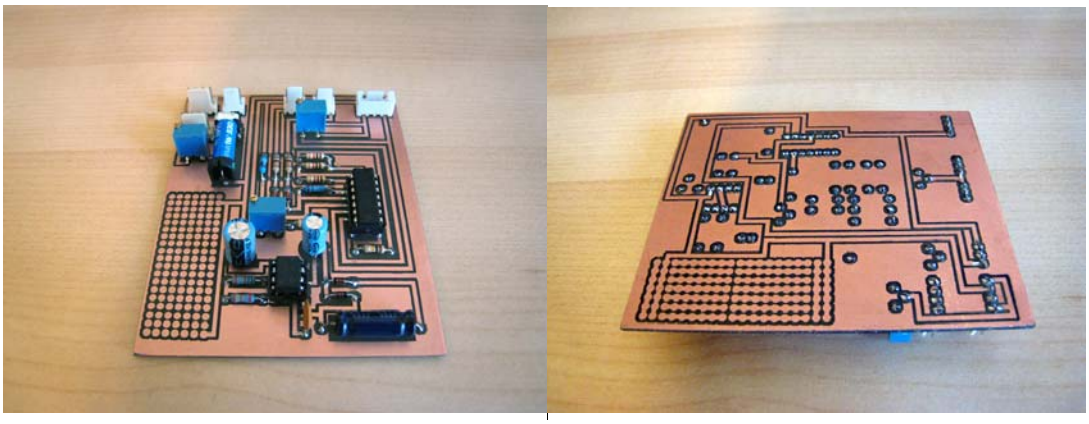

Figure 33. Fifth and final version of circuit, front (left) and back (right).

The plug size was also reduced in this circuit, compared to previous versions. Along the top edge of the front view in Figure 33, the far right plug is for the power, the next two will connect to the APDs, the next is for the final signal output, and the larger plug at the very top left will supply the laser diodes. Finally, the small plug beneath this one is for the relay switching.

- **STRUCTURAL DESIGN & PROTOTYPE DEVELOPMENT**

The completed housing of the device, as shown in Figure 34, was designed to include all of the necessary components for the system to function properly, while also maintaining a degree of portability.

Figure 34. Completed housing with components.

Encompassed in the housing are five essential components: 1) sliding tray to hold the two-well slide; 2) power supply; 3) PIC microcontroller; 4) circuit board; and 5) a complex to hold the laser diodes and avalanche photodiodes in place. Because the etching and construction of the circuit board has already been described in the *Approach* section on *Circuit Design*, these features will not be included in the following discussion. Instead, the development and implementation of the other four components will be discussed.

First, the sliding tray was made from a CD-Rom drive taken from an old computer. A CD-Rom drive was used because we wanted to limit the user's interaction with the laser diodes, APD's, and the other sensitive electrical components contained within the housing. The automated drawer-like mechanism of a CD-Rom drive enables the user run tests without physically opening the housing, as shown in Figure 35.

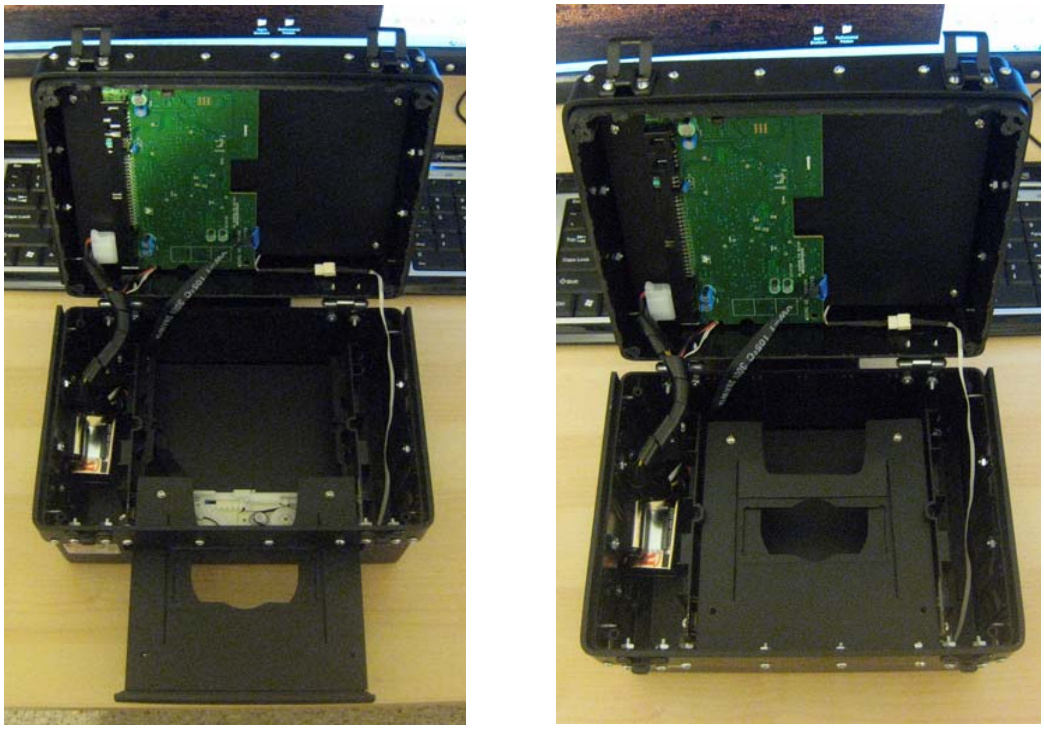

Figure 35. Open and closed positions of sliding tray mechanism.

The CD-Rom tray is wired into the power supply on the left hand side of the photo, enabling the user to open and close the tray with a push of a button that is located on the top of the case and is labeled “Open / Close.” Drilled into the top of the tray is a small piece of aluminum, which has been spray painted black to match the uniformity of the housing. The aluminum was added to make the plastic tray more rigid, as well as to make a nice square space in which the two-well slide can rest. The square space with the two finger notches was cut in to the aluminum sheet using a Dremel saw.

Although not obvious in the above figure, a small slit specified to the dimensions of the tray was also cut into the front of the housing using a Dremel saw. As with the rest of the housing, the opening fits perfectly to the dimensions of the tray so that little, if any, light will be let into the case when a test is being run. This will ensure that no problems arise from the APDs detecting external light sources and will allow the final outputs to be as accurate as possible.

Secondly, a power supply made from a 12 volt battery and a 9 volt battery was added to the housing, just to the left of the CD-Rom tray. All of the electrical components, namely the

motor to power the CD-Rom, the op-amp circuit with laser diodes and APDs, as well as the PIC microcontroller are connected to these two batteries. To limit the hassle of having to open the housing to change the batteries, a battery compartment was installed on the left side of the housing (Figure 36). This compartment may be opened with a small screw driver, and allows the user to seamlessly change the batteries should they die.

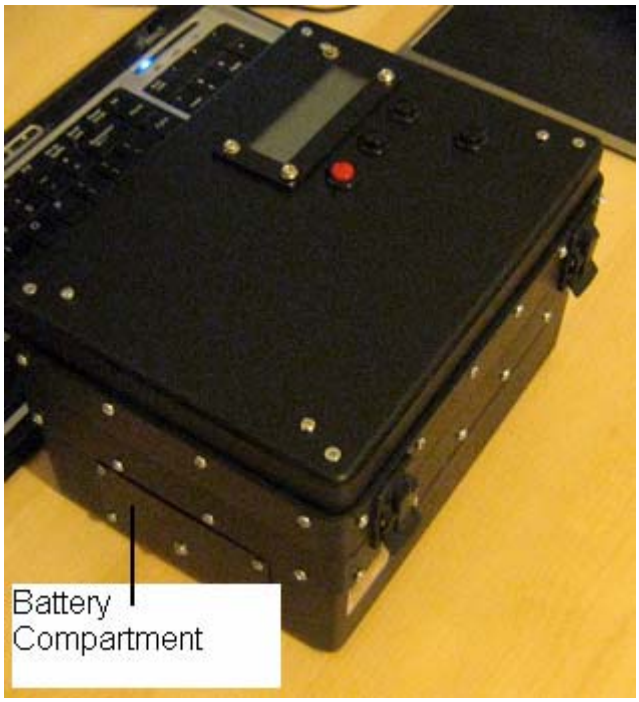

Figure 36. Side view of housing, showing power supply access.

Thirdly, a PIC microcontroller was incorporated into the housing in order to display the concentrations of *E. coli* following a successful test. The LCD of the microcontroller is visible on the top of the housing, just above the red and black buttons, as shown in Figure 37.

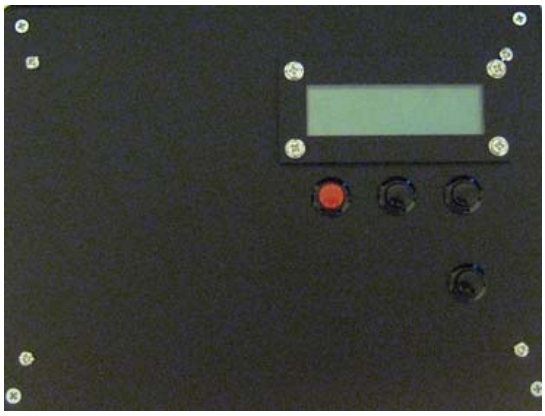

Figure 37. Top view of housing, with LCD interface.

Because the PIC microcontroller is a very expensive, delicate, and critical component of the project, we wanted to protect it from any damage should the case be opened in careless way. We also wanted to hide the microcontroller so that it would not be visible when the housing was open, mostly for aesthetic reasons. This was accomplished by attaching the microcontroller to a thin aluminum sheet which was then screwed in to the top of the housing, as seen in Figure 38.

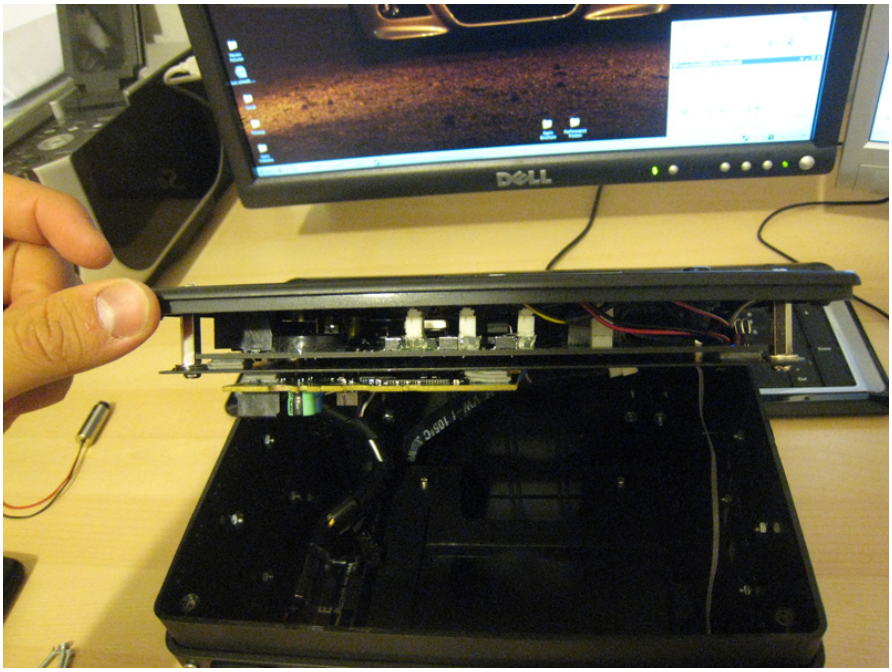

Figure 38. Aluminum sheet attaching PIC microcontroller to inner lid of housing.

Also, as shown previously in Figure 37, the switches on the PIC microcontroller were wired in to plastic buttons purchased from RadioShack, allowing the user to control and interface with the microcontroller without even seeing it or opening the housing.

Perhaps the most difficult aspect of the housing design was the development and integration of the complexes to hold the laser diodes and avalanche photodiodes. Our final design for these complexes and how they fit together is shown in Figure 39.

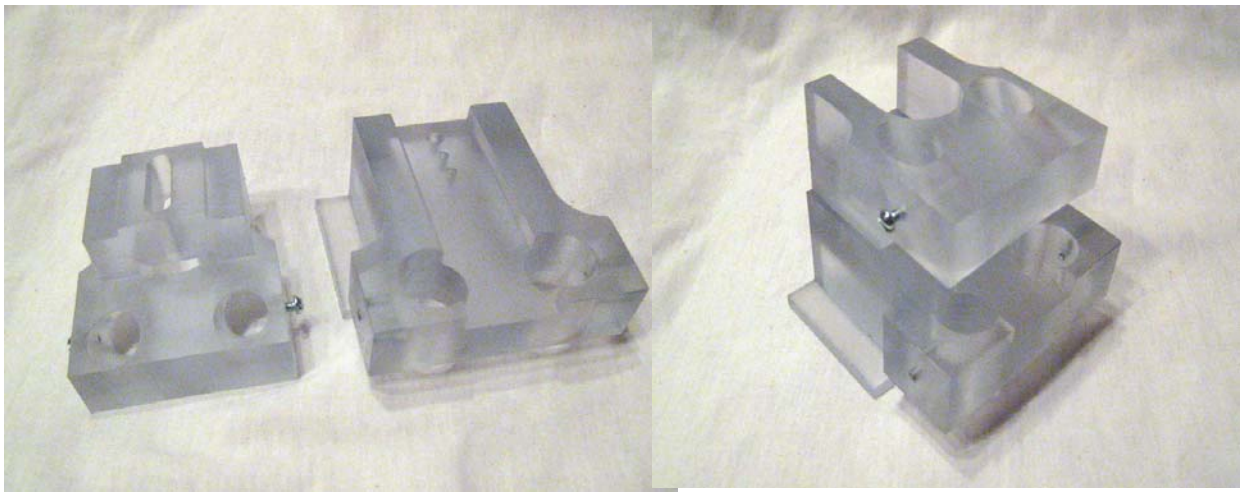

Figure 39. Support complex for the APDs and laser diodes; (a) disassembled and (b) assembled.

In Figure 39(a), the adjustable complex to hold the APDs is on the left, and the stationary complex to hold the laser diodes is on the right. The APDs fit snugly into 45 degree angled holes in the complex on the left in Figure 39(a), and the laser diodes fit into the vertical holes in the complex on the right. Screws have been added to the APD complex in order to allow the user to adjust the APDs in and out by simply loosening and tightening the screw.

Figure 39(b) shows the two complexes in their assembled form. Although it is not possible to see it from this figure, there is a long screw connecting the two complexes. This screw allows the user to move the APD complex in reference to the laser diodes by simply loosening and tightening it. As seen in the APD complex depicted on the left in Figure 39(a), a long slot has been machined into the groove where the two complexes attach, and the screw passes through this slot and into the other half of the complex. Therefore, if the user wishes to adjust the APDs forward or backward in reference to the laser diodes, he or she may loosen the screw, slide the APD complex to the desired position, and then retighten the screw. The final placement of these complexes within the housing is seen below in Figure 40. All of these parts were manufactured from Lexan polycarbonate at the ABE Shop using a mill machine, with the help and guidance of Travis Wuertz.

Figure 40. Assembled support complex, holding laser diodes and APDs, in place within the housing.

Finally, the housing itself was made from two plastic enclosures purchased from RadioShack. Although our initial design intent was to make the housing from aluminum, we found that plastic would provide the same support and rigidity as aluminum, and would be easier to work with and cheaper to produce. Two enclosures were used because we were unable to find a single plastic enclosure that was large enough to fit all of our components, yet small enough so as not to limit the portability of the device. Using a Dremel saw, we cut one of the enclosures in half, and we attached it with hinges to the top of the other enclosure. We used a Dremel saw and a drill to make the necessary holes, slits and cuts in the exterior of the housing. To limit the light that could enter the housing through the juncture where the two plastic enclosures come together, we bought two thin pieces of aluminum and bent them around the exterior of the housing before screwing them down, to create a "light-tight" seal on the housing's exterior. Two clasps were then attached to keep the housing closed when it is in use, while still allowing easy access to the inner components. The entire housing was painted with a flat black with spray paint, and is shown complete in Figure 41. For a detailed materials list and additional models of prototype parts, please refer to Appendix B.

Figure 41. Completed housing, closed position.

- **EXPERIMENTATION & RESULTS**

The prototype was tested using a laboratory-cultured *E. coli* solution to ensure that it functions properly. Because we have not had the time to conduct extensive quantitative tests, we do not know the relationship between the voltage output and the E. coli concentration. When this relationship is determined it will serve as a calibration scale, and the PIC microcontroller can be programmed to convert the voltage value to concentration value before display. Thus far our testing has been based on voltage signal only, proving the functionality of the device qualitatively, but not indicating actual *E. coli* concentration values. Further experimentation is necessary to determine the quantitative performance of the device, such as the exact detection limit and response time.

We have tested three different dilutions of E. coli solution, and have compared these results to the results of a blank test, using a standard Student's t-Test (two sample, assuming equal variances). Each of these solutions contained a high level of *E. coli*, but time constraints prohibited us from testing lower level solutions. For each test, 13 voltage readings were recorded over one minute. Three individual t-tests were carried out to compare these sets of 13 values (for each of the three solutions) to the 13 values of the blank test. Because we are only interested in determining whether the *E. coli* solutions produce a signal *higher* than the blank, a one-sided t-test was used. Critical P-value is 5%. The outcomes are summarized in Table 6, and more detailed results are available in Appendix C.

Table 6. Results of statistical t-tests.

Test (2 wells of slide)	Mean voltage signal received over 1 minute	Statistically higher than blank readings?	P-value (must be < 0.05)
Blank - Blank	2.892	----------	----------
Undiluted *E. coli* - Blank	7.411	YES	6.7×10^{-21}
½ Strength *E. coli* - Blank	5.574	YES	5.2×10^{-16}
¼ Strength *E. coli* - Blank	3.340	YES	0.0012

ETHICAL CONSIDERATIONS

There are a number of ethical issues related to the production, and use of our device which require discussion. Human health and safety is of utmost importance, and this understanding is reflected in our design.

Because this device may be used for detection of highly infectious or toxic compounds, it is designed to minimize user contact with the sample fluid. Once the sample is applied to the testing platform, it is inserted into the device where remains hidden and undisturbed for the duration of the testing period. This feature eliminates risk of inadvertently bumping an exposed sample during testing, which would not only ruin the test but also potentially contaminate the device and surrounding equipment with dangerous bacteria.

Furthermore, accurate qualitative results are absolutely essential for our device because of the infectious nature of the organisms being detected. Occurrence of false positive readings and false negatives in particular could have devastating effects. For example, if an agricultural water source is tested for *E. coli* and the device yields a false negative reading (meaning that *E. coli* is in fact present), the water will be considered safe for use on crops, and the crops may become contaminated and infect consumers with *E. coli*. The consequences of false readings would become even greater if the system were applied to detection of a more serious pathogen.

For this reason, we have taken measures to achieve the highest possible accuracy in our system. We have chosen to use an optical transducing element, which is generally one of the most accurate means of detection. However, false positives and false negatives sometimes occur in any system. Our detection method is based on scattering of light due to immunoagglutination (clumping created by antibody-target binding), so a false positive may exist if there is random clumping of the particles which was not caused by antibody-target binding. Likewise, false negatives may arise if the antibodies in the reagent solution become denatured and fail to bind to the target, or if the pathogens in the water sample are not present at a high enough concentration to warrant detection. Because of these risks, we as designers provide these precautions:

- Testing personnel should be well-instructed in proper operation of the device,
- Testers and clients should be fully informed of the potential hazards,
- Multiple tests should be carried out for confirmation before results are trusted,
- Negative test results are NOT intended to guarantee that the target pathogen is not present in levels *lower* than the system's detection limit of 100 CFU/ml.

Finally, it must be noted that we are not currently aware of any national or international standards governing production and sale of this type of device. However, before our product can be put to use in food safety, agriculture, environmental monitoring, or homeland security and military applications, it will certainly be necessary for the various organizations governing these fields to test and approve the device.

ECONOMIC ANALYSIS

- **Cost Estimate for Production**

Table 7 presents itemized costs and the total cost for production of one device.

Table 7. Itemized costs for materials and construction of prototype device.

ITEM	COST
2 silicon avalanche photodiodes, 0.5mm diameter (Edmund Optics)	2 x $109
2 close-focus laser diodes (Aixiz Lasers)	2 x $6
PIC Microcontroller and programming kit (Microchip)	$200
9-volt battery	$1
12-volt battery	$3
Printed circuit board (Elliot's Electrical Supply), and labor	$20
Wires, resistors, op-amps, etc – total cost	$20

Plastic/Aluminum casing and hardware	$50
Materials and machining for custom components	$40
TOTAL PRODUCTION COST PER UNIT	**$564**

Table 8 presents the estimated cost to carry out one assay (test) with the device.

Table 8. Costs associated with operation of device.

ITEM	COST
E. coli antibodies	$0.13/assay
Microparticles	$0.60/assay
Reagent preparation labor	$0.30/assay
Cover slips, pipette tips, reagent vials	Negligible
Two-well slides, *reusable*, 12 count (Microscope Depot)	$8 (one time cost)
Pipette	$250 (one time cost)
TOTAL REAGENT COST PER ASSAY	**$1.03**

Since no product like ours is currently available, we are unsure what the demand will be for our device once we produce it for commercial sale. We expect the market for this product to come from the fields of agriculture and food production, environmental monitoring, homeland security, military defense, and water treatment. At a sale price of $1500 per unit, we think we could sell about 30 units each year (this is a rough estimate without any real data to predict the market). We would earn $936 on each initial sale; however the more profitable aspect will be the sale of reagents. The cost of producing the antibody-coated microparticle solution for one assay is $1.03 (refer to Appendix C for calculations), but we will sell these prepared reagents at $5 per assay, yielding a profit of $3.97 per assay.

Expected product life is at least 3 years, and reagent life is 3 months. So regular users of our system will purchase reagents four times each year and will purchase a new device every three years, approximately.

- **Present Worth Analysis over 10 years**

Present worth analysis was conducted for the production and sale of these units and reagents for a period of 10 years. Complete calculations are shown in Appendix D. This analysis was based on an estimated annual interest rate of 8%, and the total profit acquired by the end of ten years has an approximate present worth of $4,081,000, which makes this an excellent investment.

However, this approximation assumes that *all* new units sold will result in sale of *additional* reagents. In reality however, a portion of the new units being sold will be replacing worn out units after their 3-year useful life, and the worn out units will no longer be requiring reagents. If this fact were accounted for in the economic calculations, it is uncertain to what extent the present worth value would decrease.

This data should only be used as a rough estimate, because we do not know how the demand for these units may increase or decrease (affecting market value), or how the state of the economy may change (affecting interest rates). Since our product utilizes cutting edge technology, a possible scenario is that once this "catches on," the market will drastically increase. On the other hand, it is possible that this system will soon become outdated or outperformed by new products, due to the rapidly evolving technology. Our design is essentially the first of its kind; therefore any assessment of the future market has a great deal of uncertainty.

CONCLUSIONS & RECOMMENDATIONS

In conclusion, we have designed and constructed a functional biosensing device for *E. coli* detection. Our system has met the initial requirements in that it is fully portable, simple to operate, has a proven performance and a short response time, and is inexpensive to build.

To achieve portability, we have designed a compact, protective housing for the system. We selected components which are small in size and do not consume a large amount of power, and we have installed several batteries within the device for onboard power supply. We also designed our system to conserve power by using an in-circuit relay to keep the lasers turned off at all times when they are not testing.

Simplicity of operation was achieved by consolidating all components within the housing, and designing the device to be completely controlled by just four buttons and a power switch. The selection of a PIC microcontroller as the system's processor allows test results and instructions to be clearly displayed to the user via an LCD screen on exterior of the device. The device is nearly entirely automated, allowing the user to simply insert a slide with the sample and blank solution, push "Test," and view the result momentarily.

The performance of our system has been proven qualitatively through collection of voltage data from *E. coli* solutions. Results were statistically analyzed to confirm that the voltages obtained from solutions containing *E. coli* are significantly greater than those obtained from a similar solution without *E. coli*. The response time of the system seems to be less than 1 minute, based on our experimentation. Much more testing is necessary, however, to quantitatively determine the response time, calibration scale, and detection limit.

This entire device was created for a cost of approximately $564, which is very inexpensive in comparison to non-portable systems with similar functions. The project objectives have been completed and design specifications have each been successfully met.

In closing we would like to offer our client several recommendations for continuation of this project, if he should choose to do so. First, we recommend that extensive tests be conducted with the prototype in order to develop a calibration scale, and that the device then be

programmed to output the value of *E. coli* concentration. Further testing can also quantitatively reveal the detection limit and the response time of the device.

Next we have two suggestions regarding adjustment of the circuit in the current design. We recommend adding a second op-amp element and connecting the op-amps in parallel with the APDs, rather than having both APDs connect to one op-amp. This will avoid complications and signal fluctuations due to the single op-amp's attempts to equalize the signals coming from the two APDs. Also, in the current design, the two laser diodes draw power from the same source. The potentiometer controls the amount of voltage they receive, but because of variation between the two lasers, one may produce a more intense light beam than the other, given the same voltage. We recommend implementing an independent voltage regulation portion for each of the two laser diodes.

Finally, in regards to the long term scope of this design, we recommend implementing a more advanced sensing platform, such as the microfluidic devices currently in use for lab-on-a-chip biosensors. The pressure-driven microchannel flow would require additional automated components with the system, adding to the complexity and power requirement. However, a microfluidic platform would not require the "messy" handling of reagents on a slide, making the system even more user-friendly. Most likely a lower detection limit would be obtained and risk of error would decrease. Eventually, our design could even be expanded and tailored to detect a variety of different organisms simultaneously, through the use of a multichannel microfluidic platform.

REFERENCES

DexCom. 2007. The seven system. DexCom™, Inc. Available at: http://www.dexcom.com/html/dexcom_products.html. Accessed 10 October 2007.

Han, J. H., B. C. Heinze, J. Y. Yoon. 2008. Single cell level detection of Escherichia coli in microfluidic device. *Biosensors and Bioelectronics* 23:1303-1306.

Lucas, L. J., J. H. Han, J. Chesler, J. Y. Yoon. 2007. Latex immunoagglutination assay for a vasculitis marker in a microfluidic device using static light scattering detection. *Biosensors and Bioelectronics* 22: 2216–2222.

Marler-Clark. 2007. About E. Coli: E. coli O157:H7. Available at: http://about-ecoli.com/. Accessed 18 November 2007.

Marmonier, S. and C. Flyckt. 2002. *Photomultiplier Tubes: Principles and Applications.* Brive, France: Philips Photonics.

Martel Meters. 2007. Products. Martel Electronics Corporation. Available at: http://www.martelmeters.com/products. Accessed 17 November 2007.

Medtronic. 2007. Guardian® REAL-Time. Medtronic MiniMed, Inc. Available at: http://www.minimed.com/products/guardian/. Accessed 10 October 2007.

Microchip. 2007. Products. Microchip Technology, Inc. Available at: http://www.microchip.com/. Accessed 26 November 2007.

Ocean Optics Inc. 2007. Products. Ocean Optics, Inc. Available at: http://www.oceanoptics.com/Products.asp. Accessed 1 October 2007.

Pathogen Detection Systems. The PDS Solution. 2004-2006. Pathogen Detection Systems, Inc. Available at: http://www.pathogendetect.com/products.php. Accessed 26 November 2007.

CDC. 2006. Disease Listing: Escherichia coli O157:H7. Centers for Disease Control and Prevention. Available at: http://www.cdc.gov/ncidod/dbmd/diseaseinfo/escherichiacoli_g.htm. Accessed 28 November 2007.

Research International. 2007. Raptor^{TM} 4-channel bioassay system. Research International, Inc. Available at: http://www.resrchintl.com/raptor-detection-system.html. Accessed 8 October 2007.

Seattle Sensor Systems. No date. Products. Seattle Sensor Systems, Inc. Available at: http://www.seattlesensors.com/products.htm. Accessed 8 October 2007.

Yoon, J. Y. 2007. Latex Immunoagglutination Assay in Lab-on-a-Chip. *Biological Engineering* 1: 79-94.

APPENDIX A: DESIGN CRITERIA & CONSTRAINTS

Performance –

Device should be sturdy enough to hold up to wear and tear from daily use and frequent transportation. It should have an adequate built-in power supply to run up to 100 tests before recharging is necessary. It should function correctly in a wide range of environments, including temperature and humidity extremes, and various light levels.

Life in Service –

Useful life should be 2 years at minimum, under heavy use. We will select optimal materials and design the system so as to achieve the longest possible service life. The system will not have a limited "shelf life," although fresh reagents must be supplied every 3 months. In general, if the device is not in use or it is under minimal use, its useful life will be extended.

Safety –

Because this device may be used for detection of highly infectious or toxic compounds, it should be designed in such a way as to minimize user contact with the sample fluid. Occurrence of false readings (particularly false negatives) should be extremely rare, and users are to be informed of the potential risks, as well the proper operating procedures and precautions.

Accuracy and Reliability –

When operated properly, we expect this system to be accurate, producing test results that are within ± 10% of the actual value of target in a sample. The lower detection limit should be below 100 cfu/ml. False positive results should occur in no more than 5% of tests, and false negatives even less frequently (< 1 %).

Standards and Specifications –

To our knowledge, there are no national or international standards governing production of this type of device. However, before our product can be put to use in food safety, agriculture, environmental monitoring, or homeland security and military applications, it will certainly be necessary for the various organizations governing these areas to test and approve the device.

Physical Characteristics –

We intend to minimize the size and weight of our system, in order to broaden the field of potential applications. While we are unsure of what dimensions we can practically achieve, we expect that the final product will be the appropriate size and weight to be easily carried with one hand.

Ergonomics –

The device will be designed for use by hand while resting on a surface. Any components of the system which must be mechanically moved by the user will have appropriate handles, knobs,

buttons, or holes. Because of the small size of the device, however, these features may still require careful manipulation with the fingertips. The device will likely include a protective cover or case for ease of transport. Overall, user input will be minimal and simple.

Materials and Assembly –

The external portion of the system will be constructed of materials which are lightweight yet strong and durable. The interior must contain delicate wires, electrical components, and glass; therefore it must be positioned securely and well-protected by the external housing. The pipettes and bottles of reagents required for running tests will be isolated from the device, but the system's carrying case will include a secure place for these.

Aesthetics –

Complex circuitry and working components with be hidden within the device, so that the user interface is simple and inviting. For testing, the chip with sample and reagents applied will be inserted entirely into the device, where it cannot be seen or disturbed during a test.

Competition –

While there is no existing product exactly like the one we are designing, there are a variety of biosensors created for research which function by similar means (immunoagglutination and optical detection). We will compare our biosensing setup and results with these. There are also other types of biosensors which have been condensed and marketed as a portable device. We will compare the portability of our system to these.

Target Product Cost –

We hope to be able to produce and sell our complete system for $1000 or less. We will also supply our clients with reagents, and we will sell these at approximately $5 per assay, which will yield a significant profit.

Production Quantity –

Since no product like ours is currently available, we are unsure what the demand will be for our device once we produce it for commercial sale. Expected product life is at least 3 years, and reagent life is 3-6 months. So regular users of our system will purchase reagents a few times each year and will purchase a new device every several years. As a rough estimate (without any real data to base it on), we expect to sell about 50 units each year.

APPENDIX B: MATERIALS LIST & PROTOTYPE PARTS

The prototype circuit required the following materials:

- 1 – Copper Circuit Board
- 1 – Bottle of Ferric Chloride
- 1 – 24K ¼ Watt Resistor
- 1 – 56K ¼ Watt Resistor
- 1 – 3300pF 25V Ceramic Capacitor
- 1 - 47uF 25V Electrolytic Capacitor
- 1 - 10uF 25V Electrolytic Capacitor
- 1 - 100uF 25V Electrolytic Capacitor
- 2 - 1N4148 Silicon Diode
- 1 – 555 Timer
- 2 – Silicon 0.5mm UV/VIS Avalanche Photodiodes
- 2 – 635 nm 5mW Laser Diodes
- 3 – 20K potentiometers
- 1 – LM324 Operational Amplifier
- 1 – 9V battery
- 1 – 12V battery
- 4 – 1KΩ Resistors
- 2 – 10KΩ Resistors
- 1 – 100KΩ Resistors
- 2 – 500KΩ Resistors
- 2 – Diodes
- 1 – Relay Switch
- 1 – Picdem 2 Plus
- Various male/female connectors

The prototype processor and programming aids consisted of:

- 1 – PICDEM 2 Plus PIC microcontroller
- 1 – MPLAB in-circuit emulator
- 1 – MPLAB ICD 2 (in-circuit debugger)

The prototype housing and structure required the following materials:

- Various Wires and connectors
- Assortment of screws and nuts
- Various buttons and switches purchased from RadioShack
- 1 – Sheet of Aluminum
- 1 – Block of Lexan polycarbonate
- 1 – Can of *Flat Black* spray paint
- 1 – CD-Rom drive with electric motor and tray
- 2 – metal hinges
- 2 – metal buckles

The following CAD drawings depict the parts purchased or fabricated for construction of the prototype:

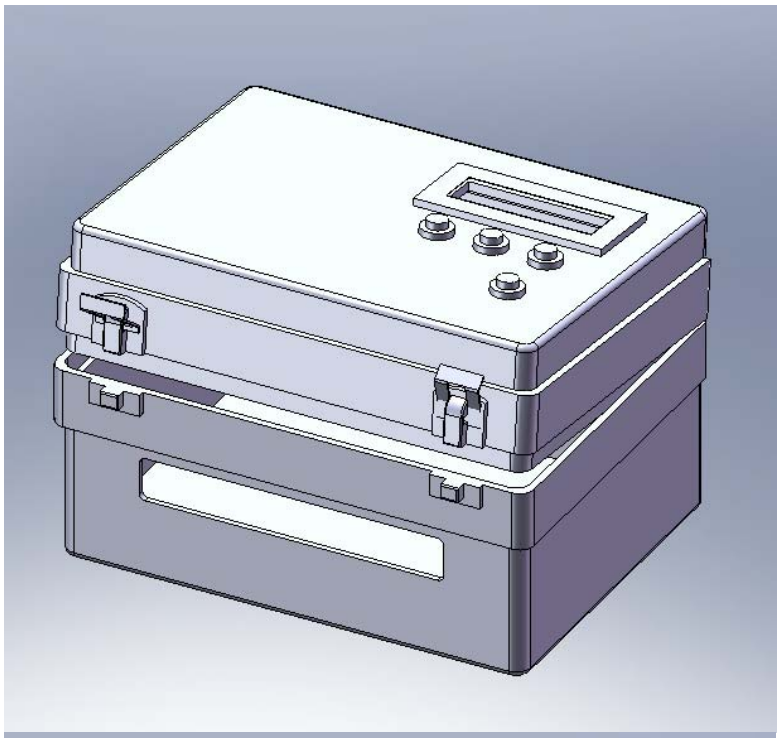

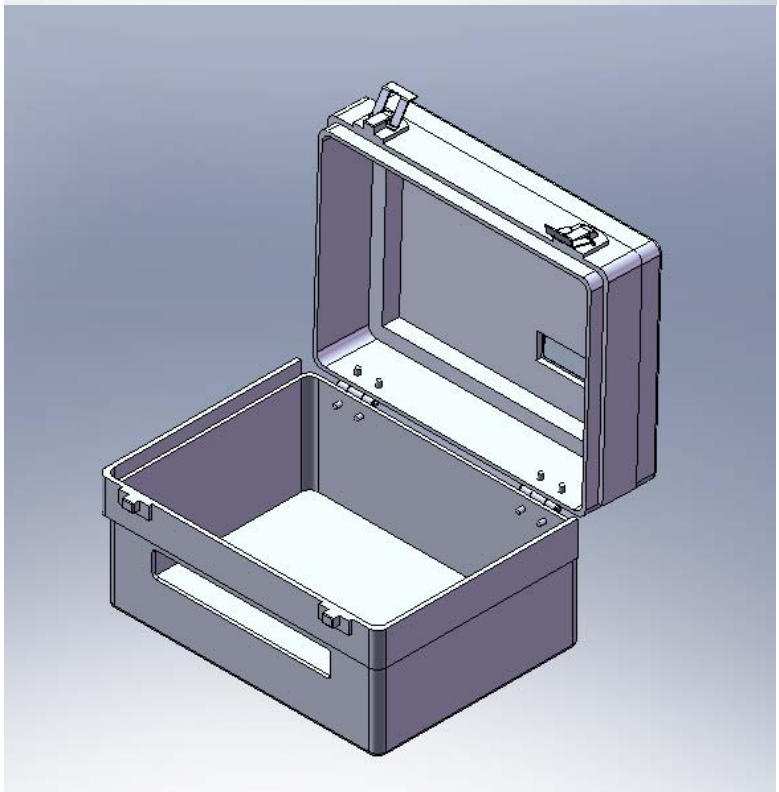

HOUSING

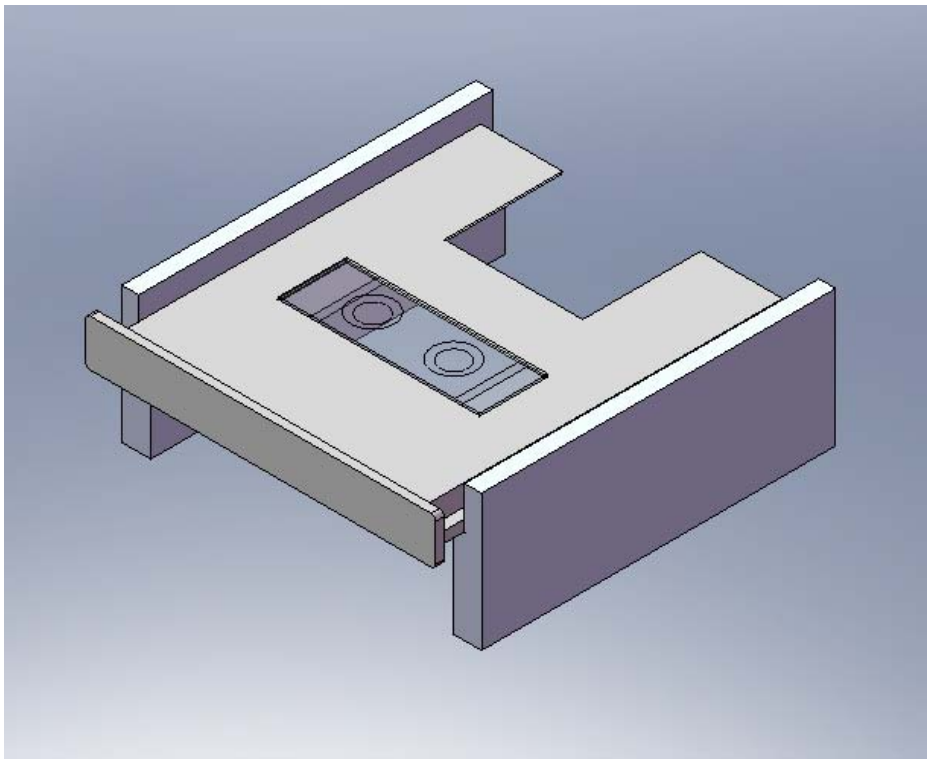

SLIDING DRAWER WITH TWO-WELL SLIDE

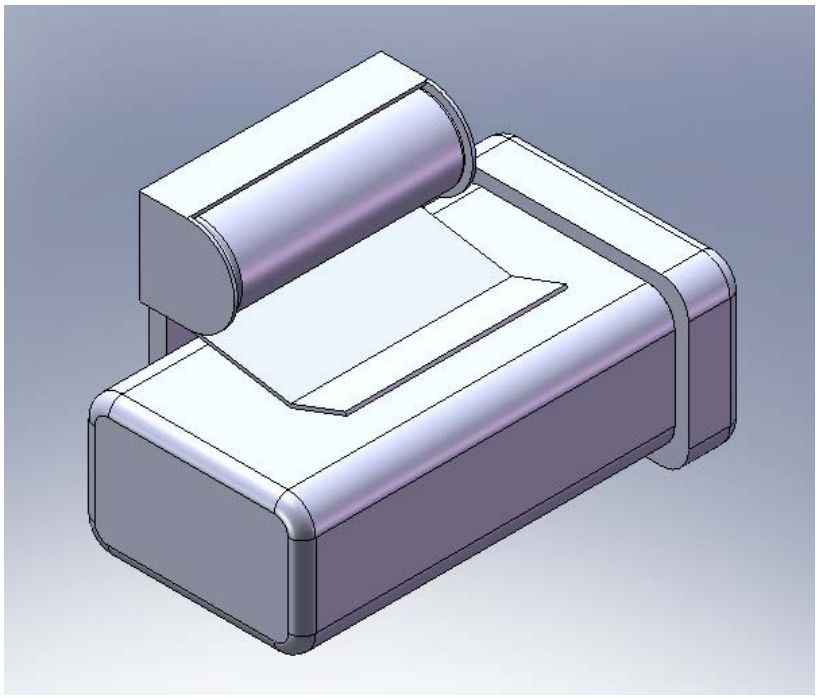

BATTERY ASSEMBLY

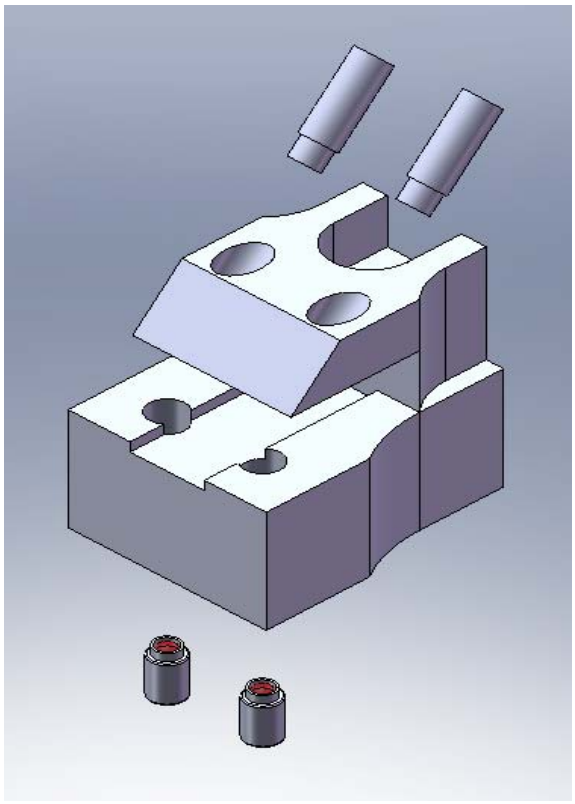

MOUNT ASSEMBLY WITH LASERS AND APDS

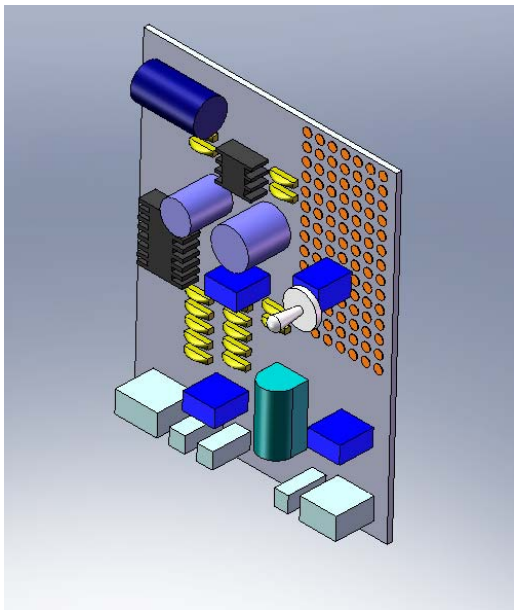

CIRCUIT BOARD

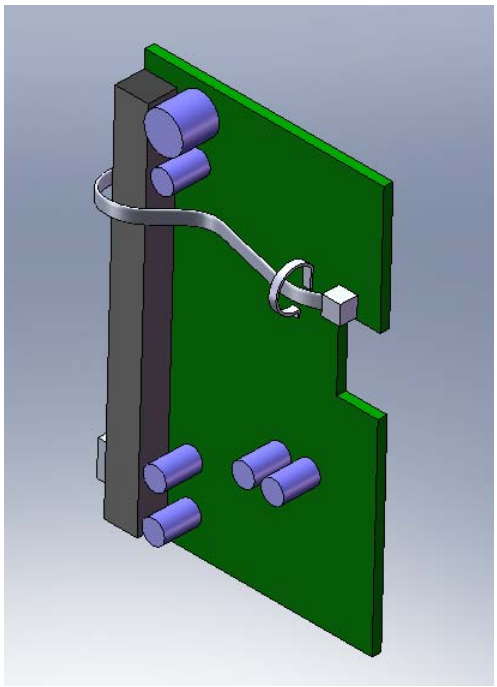

CONTROLLER BOARD FOR MOTORIZED DRAWER

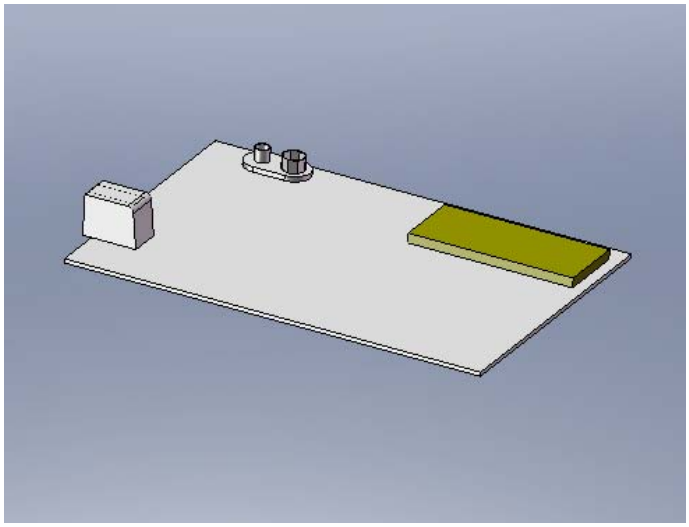

PIC MICROCONTROLLER

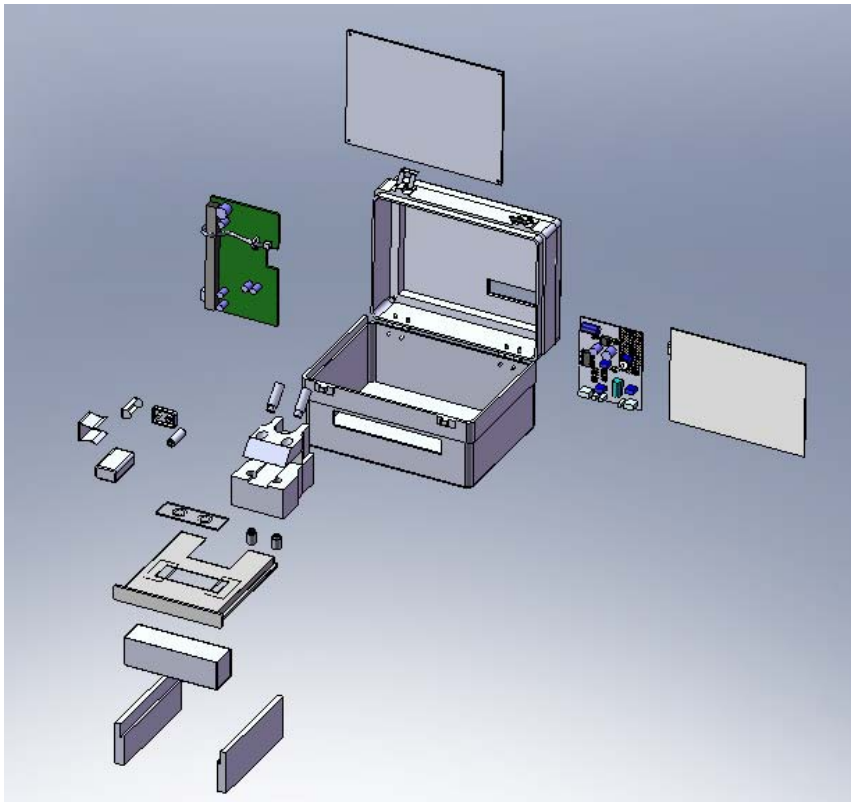

EXPLODED ASSEMBLY VIEW

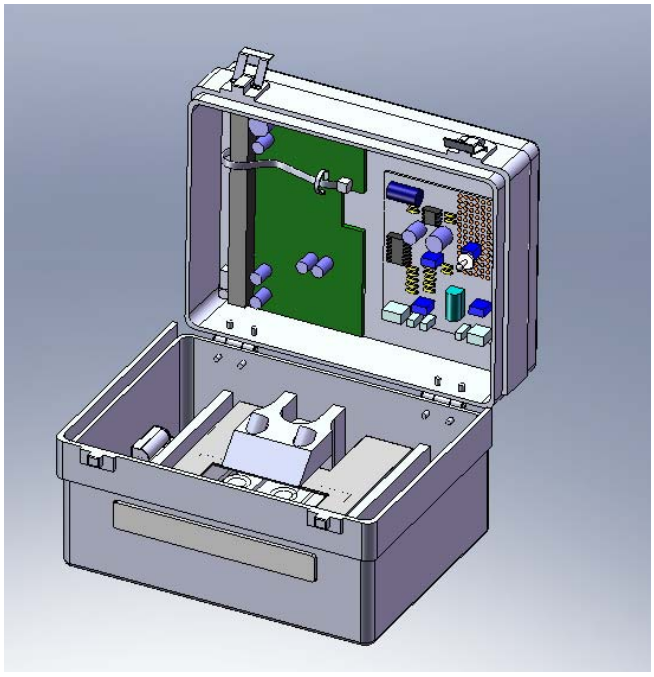

COMPLETE ASSEMBLY

APPENDIX C: EXPERIMENTAL RESULTS

Following are the voltage data collected for testing of three *E. coli* solutions and a blank.

VOLTAGE DATA COLLECTED	Reading #	Blank - Blank	Undiluted E. coli - Blank	One half E. coli - Blank	One quarter E. coli - Blank
	1	3.57	7.75	5.45	3.02
	2	2.74	7.53	5.41	3.43
	3	2.55	8.29	5.53	3.31
	4	2.24	7.26	5.11	3.79
	5	2.89	7.38	5.38	3.33
	6	2.8	7.56	5.56	3.41
	7	2.81	7.15	5.36	3.26
	8	2.94	6.97	5.66	3.2
	9	3.02	7.53	5.95	3.21
	10	3.26	7.24	6.18	3.22
	11	3.42	7.11	5.31	3.06
	12	3.2	7.19	6.06	3.46
	13	2.16	7.38	5.5	3.72
MEAN:		**2.892**	**7.411**	**5.574**	**3.340**
STANDARD DEV:		0.419	0.341	0.312	0.226

The results of the t-tests for each of the three samples, performed using Microsoft Excel, are shown below.

t-Test: Two-Sample Assuming Equal Variances

	Blank - Blank	*One quarter E. coli - Blank*
Mean	2.892307692	3.34
Variance	0.175302564	0.051116667
Observations	13	13
Pooled Variance	0.113209615	
Hypothesized Mean Difference	0	
df	24	
t Stat	-3.392303131	
P(T<=t) one-tail	**0.001201304**	
t Critical one-tail	1.710882067	
P(T<=t) two-tail	0.002402608	
t Critical two-tail	2.063898547	

t-Test: Two-Sample Assuming Equal Variances

	Blank - Blank	*One half E. coli - Blank*
Mean	2.892307692	5.573846154
Variance	0.175302564	0.097542308
Observations	13	13
Pooled Variance	0.136422436	
Hypothesized Mean Difference	0	
df	24	
t Stat	-18.50963304	
P(T<=t) one-tail	**5.15174E-16**	
t Critical one-tail	1.710882067	
P(T<=t) two-tail	1.03035E-15	
t Critical two-tail	2.063898547	

t-Test: Two-Sample Assuming Equal Variances

	Blank - Blank	*Undiluted E. coli - Blank*
Mean	2.892307692	7.410769231
Variance	0.175302564	0.116174359
Observations	13	13
Pooled Variance	0.145738462	
Hypothesized Mean Difference	0	
df	24	
t Stat	-30.17589625	
P(T<=t) one-tail	**6.70815E-21**	
t Critical one-tail	1.710882067	
P(T<=t) two-tail	1.34163E-20	
t Critical two-tail	2.063898547	

APPENDIX D: ECONOMIC CALCULATIONS

Reagent Cost per Assay

The significant costs associated with production of reagents are the costs of the antibodies and microparticles and the cost of labor. Buffer for use as the control solution, vials for storing reagents, and pipettes for transferring reagent are inexpensive, and their cost has been neglected. Thus the cost of reagents is found in this way:

[The microparticles and antibodies are considered to be spherical particles.]
Microparticle diameter = 0.92 μm

- ⇨ Volume = $(4/3)\pi r^3 = 3.2617\ \mu m^3$
- ⇨ Surface Area = $4\pi r^2 = 10.636\ \mu m^2$

Antibody diameter = 0.01 μm

- ⇨ Volume = $(4/3)\pi r^3 = 4.1888 \times 10^{-6}\ \mu m^3$
- ⇨ Cross-sectional Area = $\pi r^2 = 3.1415 \times 10^{-4}\ \mu m^2$

Approximately 1/3 of the bead surface will be covered by antibodies.

Number of antibodies per microparticle:

(1/3)(microparticle surface area) / (antibody area) = $(1/3)(10.636\ \mu m^2) / (3.1415 \times 10^{-4}\ \mu m^2)$

= 11286 antibodies per microparticle

Each well in the two-well slide will contain 35 μl of microparticle-antibody conjugate solution, at 2% particles by volume. Each assay requires 2 wells (negative control and sample). We will sell reagents in single-assay vials, so we will include an extra volume of solution in order to secure it in the vial. Therefore, 100 μl of microparticle-antibody conjugate solution will be required per assay. (One microliter is equal to $10^{-9}\ m^3$ or $10^9\ \mu m^3$).

Volume of antibody-bound microparticles required per assay:

100 μl (0.02)(10^9 μm^3/ μl) = 2 x 10^9 μm^3

Number of antibody-bound microparticles required per assay:

Volume of particles required / volume per particle

= Vol. of particles required / (vol. microparticle + vol. Ab* number of Ab per microparticle)

= 2 x 10^9 μm^3/ (3.2617 + 4.1888 x 10^{-6} x 11286) μm^3 = 6.0442 x 10^8 particles per assay

E. coli antibodies cost $300 for 1 ml, at a concentration of 4 mg/ml. The molecular weight of the antibodies is 150000 g/mol = 0.15 x 10^9 mg/mol.

Cost of antibodies per assay:

($300/ml Ab)(1 ml/4 mg)(0.15 x 10^9 mg /mol)(1 mol/6.022 x 10^{23})(11286 Ab/particle)(6.0442 x 10^8 particles/assay)

= $0.1274/assay

The antibodies for one assay can be obtained for as little as 13 cents.

Microparticles cost approximately $150 for 5 ml, containing 10% solids by volume. As shown above, the volume of one microparticle is 3.2617 μm^3, and one assay requires 6.0442 x 10^8 microparticles. (One milliliter is equal to 1 cm^3 or 10^{12} μm^3)

Number of microparticles purchased for $150:

(5 ml)(10^{12} μm^3/1 ml)(0.10)(1 microparticle/3.2617 μm^3) = 1.533 x 10^{11} microparticles

Number of assays carried out with $150 worth of microparticles:

1.533×10^{11} microparticles / 6.0442×10^{8} microparticles per assay = 253.6 assays

Cost of microparticles per assay:

$150 / 254 assays = $0.591 per assay

The microparticles for one assay can be obtained for 60 cents.

The labor associated with making the antibody- microparticle conjugate is approximately 3 hours to make enough conjugate for 100 assays.

Cost of labor per assay:

(3 hr/100 assays)($10/hr) = $0.30 per assay

The labor to make reagents for one assay will cost 30 cents.

Therefore the total cost of reagents per assay is $1.03.

Present Worth of Production and Sales over 10 Years

Time increment *N* is 1 year. All annual profits are lumped into one year-end payment.
Analysis is conducted over 10 years, with initial production being time zero.
Interest rate *i* is 8% per year.

A single unit costs $564 to produce and we will sell it for $1500. Therefore profit per unit is $936. We expect to sell 30 units per year, giving us an annual profit of $28,080 for sale of the units.

A single vial (one assay) of reagents costs $1.03 to produce and we will sell it for $5. Therefore profit per assay = $3.97. We expect to sell 1000 vials per year, for each unit that has been sold. So the base annual profit for sale of reagents is $3.97 per vial*1000 vials*30 units = $119,100.

However, since 30 additional units are sold each year, the profit due to sale of reagents will *increase* by this amount every year.

Profit from the units and the base annual profit from the reagents is represented as a uniform series cash flow (we are paid $28,080 + $119,100 = $147,180 each year for ten years). The additional profit from the reagents is represented as an arithmetic gradient series cash flow (the amount we are paid increases by $119,100 each successive year).

Therefore the present worth of our whole investment is simply the sum of the present worth of the uniform series cash flow and the present worth of the gradient series cash flow.

$P = P_{uniform} + P_{gradient} = A*[P/A, i, N] + G*[P/G, i, N]$

where A = $147,180; G = $119,100; i = 8%; and N = 10 years.

$= A*((1+i)^N - 1) / (i*((1+i)^N)) + G*((1+i)^N - N*i - 1) / ((i^2)*(1+i)^N)$

$= \$987,590 + \$3,093,840 = \$4,081,430$

Present worth of profit from the sale of our product over ten years is nearly $4.1 million, an excellent investment. (Note: This approximation assumes all new units sold will result in additional sale of reagents. In reality however, a portion of the new units being sold will be replacing worn out units after their 3-year useful life, and the worn out units will no longer be requiring reagents.)